A Delayed Takagi–Sugeno Fuzzy Control Approach With Uncertain Measurements using an Extended Sliding Mode Observer

Muhammad Shamrooz Aslam[1,2], **Prayag Tiwari** [3,*], **Hari Mohan Pandey** [4,*], **Shahab S. Band.** [5,*], **Hesham El Sayed** [6]

Abstract

In this study, a *sliding mode observer (SMO)* is implemented on a T–S fuzzy system with multiple time–varying delays over continuous time. Because state data may not be fully available in practice, state observers are used to estimate state information. A system based on observers is implemented with *non–parallel distribution compensation (N-PDC)*. Moreover, the concept of dissipative control provides a framework for analyzing the performance of H_∞, $L_2 - L_\infty$, and dissipativeness. In order to design two sliding surfaces using the *SMO* gain matrix, first two integral–type sliding surfaces must be constructed. Then, we define a few additional parameters using fuzzy Lyapunov stability and *SMO* theory, resulting in asymptotically stable closed–loop performances. On the basis of the new error system, convex optimization is used to generate the sliding mode controller and the gained weight matrices. Following is an example of the *power system* (ship electric propulsion) to demonstrate the potential scheme.

Keywords: Fuzzy Lyapunov–Krasovskii Functions, Sliding mode control, Time–delay system, Dissipative analysis.

1 Introduction

Along with the rapid development of digital technology, *networked control systems (NCSs)* have garnered substantial attention in recent years because of their widespread industrial applications in areas of automation, robotics, process control, and so on [1]. A key feature of *NCS* is that the control components are distributed and connected through an interactive communication network [2]. Unlike traditional dedicated point-to-point communication, *NCSs* have several advantages including low cost, ease of setup, and high reliability [3]. Nevertheless, the addition of the communication network leads to a series of challenging problems such as network delay, insufficient bandwidth, ineffective connections, and so on, which may degrade the performance of the system or cause system instability [4]. Recently, much effort has been made in examining stability, estimation, filtering, and control problems in *NCS* and many achievements have been reported, see [5, 6] and references therein.

Up to now, many control problems of *NCSs* have been studied in the literature [7]. However, most of these results rely on the conventional transmission paradigm, which is impractical and leads to extreme consumption of

*Corresponding author. *Email addresses:* H.M. Pandey, P. Tiwari, S.S. Band.

1. Artificial Intelligence Research Institute, China University of Mining and Technology, Xuzhou, China. Email addresses: shamroz_aslam@gxust.edu.cn (M.S. Aslam)

2. School of Automation, Guangxi University of Science and Technology, Liuzhou 545006, China.

3. School of Information Technology, Halmstad University, Sweden. (email: prayag.tiwari@ieee.org)

4. Data Science & Artificial Intelligence Department, Bournemouth University, Fern Barrow, Poole, Dorset, BH12 5BB, UK. (email: pandeyh@edgehill.ac.uk)

5. Future Technology Research Center, College of Future, National Yunlin University of Science and Technology, 123 University Road, Section 3, Douliou, Yunlin 64002, Taiwan, ROC. (email: shahab@yuntech.edu.tw)

6. H.E. Sayed College of Information Technology, United Arab Emirates University, Abu Dhabi 15551, United Arab Emirates. (email:helsayed@uaeu.ac.ae)

communication resources. Hence, under the circumstances, it is significant to exploit a novel transmission paradigm that can reduce the communication burden in *NCS* while ensuring system performance. Recently, *event-triggered mechanisms (ETMs)*, as an alternative to the conventional time-triggered scheme, have been proposed to mitigate the communication burden [8]. Compared with the conventional time-triggered periodic scheme, the transmission rate of channel resources can be greatly decreased in *ETM* even further because the network channel is only activated when deviations between the latest data and the current sampling signal exceed pre-established thresholds. Therefore, *ETM* has received extensive attention and many outstanding achievements have been attained. For example, adaptive control of *ETM* is examined as a method to stabilize uncertain nonlinear systems in [9]. Based on an *ETM*, the design of the H_∞ control protocol for the T–S fuzzy system is investigated in [10]. The results showed a significant reduction in communication burden. Furthermore, when considering practical factors such as component ripening, exterior interference, and unexpected environmental noises, the ambiguity that occurs in the measured output cannot be overlooked [11]. Readers can refer to [12] to further explore the new horizons of nonlinear models, such as neural networks, fuzzy systems, and optimization methods.

On another research front, *sliding mode control (SMC)*, as an effective robust control method has been extensively employed in many complex systems due to its outstanding advantages including strong robustness to uncertainty, system nonlinearity, and disturbances [13]. Owing to the above characteristics, *SMC* has demonstrated excellent performances in the variability of systems including multi-agent systems, and singularly perturbed systems [14]. The general principle of *SMC* is to achieve system stability by using the effect of designed laws on switching surfaces, which promotes stability and performance [15]. So far, *SMC* techniques have received much attention and many valuable achievements have been reported [16]. For instance, the authors examined output feedback control for *SMC* problems in [17]. In [18], *SMC* strategies are applied to estimate unknown parameters. A fuzzy *SMC* strategy is developed for utilizing the maximum wind power [19]. In addition, *SMC* results have been presented for a wide range of uncertain systems, notably for high-order control systems. In [20], the dissipativity of *SMC* with respect to time-delayed T–S fuzzy particular systems is studied. Taking into account input and state delays, authors in [21] analyzed the *SMC* of fractional-order systems. An algorithm for tracking discrete-time uncertain systems is provided in [22]. On the other side, fuzzy *SMC* schemes are suggested by the authors using exponential functions for uncertain nonlinear systems [23]. The authors in [24] investigated the type of linear systems with appearing of time-varying inputs and states, however, it does not consume time delay into account for analyzing the system. This fact leads to the present study.

In addition, it is well known that the state information in the systems is not always available in reality due mainly to limited environmental conditions, and in some cases, it is impossible to correspond to real physical quantities that indicate its state. As an alternative method, sliding mode observer *(SMO)* has been gradually applied to cope with the system state estimation in recent years. In fact, the design of *SMO* is implemented through the SMC approach [25]. Accordingly, *SMOs* have better resilience to uncertainty, nonlinearity, and disturbances as compared to *SMCs* [26]. So far, *SMO* design has been extensively investigated over the last few decades, including studies of stochastic systems [27], T–S fuzzy systems [28], and many more. To cite a few, a stochastic exponential stability problem for neural networks was investigated using the observer-based event-triggered *SMC* process in [29]. Also, *SMC* approaches are used to analyze a fractional-order T–S fuzzy system observer in [30], whereas a higher-order under balances matrix approach is used to research discrete-time T–S systems in [31]. In [32], authors developed a disturbance observer based on an integral *SMC* technique to address the H_∞ control problems in the unknown-uncertain-and-mismatched disturbances. On the other side, *extended sliding mode control (ESMC)* has attained significant results, especially in the power sector. In [33], authors explored the *SMC* for the power application with their extended states, while in [34], adaptive *ESMC* is investigated for the neural networks with disturbance rejection. As a result, there is a need for further research to determine the properties of *ESMC* in the power engineering sector. These findings motivate the research in this paper.

On the other hand, researchers cannot ignore the impact of nonlinear terms, which always result in plant instability. To adequately tackle the nonlinearities, effective strategies have been developed recently. For example, using an

adaptive ETM, authors in [35] investigated the stabilization problems of nonlinear systems that are uncertain. In [36], a communication scheme was explained using the event-triggered protocol which was developed for *T–S fuzzy systems*. In addition, the uncertainty occurring in the measured output cannot be ignored if practical factors are taken into account, such as the aging of the components and external interferences [37]. In particular, it is well known that *SMO* has nonlinear input in addition to linear input as compared to *SMC*, which is necessary to ensure finite time movement of the system's state motions [38]. However, in this context, there are only very few results for the nonlinear terms that appear in *SMO* design for *delayed T–S systems*, which motivates us to enrich this aspect in this paper.

In the same consequences, system stability and performance can be impacted by external disturbances and uncertainties. The performance indices can help to improve the measurement of system stability with the analysis of the system. Several performance measures are frequently used, including passivity performance [39], and standard dissipativity [40]. Scholars have recently tried to unify several different performance measures under one framework, allowing them to design more robust and flexible control systems. In [41], authors discussed four performance indices under one framework called extended dissipative performance. Based on this result, extended dissipative processes have been applied to a variety of systems analyses [42]. Despite the fact that limited work has been done in this area, though, the measure of state information and uncertainties regarding measurement have also been not taken into account in terms of determining *SMC* for nonlinear systems with extended dissipative performance. As a result, the objective of this article is to address these issues.

2 Related Work

In the theoretical analysis and practical application of dissipative control, *SMC* is one of the most popular control methods available today due to its insensitivity to robustness, external disturbances, and active response speed. It has been proven to be an excellent control method for all types of nonlinear systems. In [39], the authors present a *hidden Markov model (HMM)* to address the dissipative control problem over finite time. In this research, an *HMM* is introduced to present the asynchronous problem between the control protocol and the system. Based on *HMM*, a finite–time asynchronous control protocol is developed for continuous–time *MJSs* under strictly dissipative performance and *Lur'e nonlinearity*. The stability of this problem is analyzed by applying *linear matrix inequality* and *Lyapunov theory*, where sufficient conditions were derived to ensure the finite–time boundedness of the resulting system. On the other side, the practical significance of this design is demonstrated by a wind turbine system conducted by stochastic wind speed. In the above–mentioned literature, [8, 16, 19, 24, 25], the authors examined the new terms of sliding mode control in the form of linear matrix inequalities. In most of the studies investigated, many researchers explored the common Lyapunov function which does not contain all plant information. As a result, conservatism may increase. In this regard, we investigated the new fuzzy Lyapunov function. Therefore, introducing membership–function-dependent integral terms to the fuzzy Lyapunov function would be of significant interest. In contrast, there has been significant evidence in studies of sliding mode control with observer-based control [13, 26, 27, 32, 33]. It should be pointed out that the observer–based control designed in the aforementioned works does not have time delays. In practice, the observer's state itself may contain time delays in its states. The input of the plant may be a delayed signal measured from the output, especially when considering the environment of the communication channel [29]. By considering these features, the authors present the scientific solution to delayed observation–based control for sliding mode control.

In light of the discussion above, the primary purpose of this study is to investigate the *SMC* issue for continuous-time nonlinear systems with dissipative properties. Moreover, this article is significant for the following three aspects:

1. New error systems with *SMO* systems are developed by constructing two integral–type sliding surfaces in which *SMO* gain matrices $\mathcal{L}_i$ were involved. Using a continuous-time nonlinear system as an example, the authors address the *SMO* problem in the first attempt. In this study, the multiple delays in both state information

and observer state can also be considered.

2. Also in this article, we established *SMC*-based *SMO* strategies in the presence of the system's delay. Furthermore, an analysis of the performance of H_∞, $L_2 - L_\infty$, dissipativity and passivity within a unified framework is provided by a concept of dissipative control.

3. By using the new *fuzzy Lyapunov function* with mode-dependent properties, the analysis of the extended dissipative performance is considered. In order to increase the comprehensiveness and generality of analysis results, the scalar and weighting matrices can be adjusted to convert the extended dissipative performance into four standard performance indices.

Notations: The notations used in this article are general, and a majority of them are commonly used in published literature. In specific, throughout this paper, we use the presentation of matrices $\mathcal{X}_i \geq \mathcal{Y}_i$ for real symmetric matrices $\mathcal{X}_i$ and $\mathcal{Y}_i$. The integrable vector functions over $[0, \infty)$ are represented by $\mathcal{L}_2[0, \infty)$. $\otimes$ is denoted as the Kronecker product. "$(\bullet)$" indicates a term that is determined by symmetry with an ellipsis. A matrix I with proper dimensions is called an identity matrix.

3 Problem Statement with System Description

In this article, our focus is on delayed T–S fuzzy systems [25] described by

Fuzzy rule i : **IF** $\bar{\vartheta}(t)$ is $\bar{W}_{i1}$ and $\cdots$ and $\bar{\vartheta}_g(t)$ is $\bar{W}_{ig}$, **THEN**

$$\begin{array}{rcl} \dot{m}(t) & = & \mathcal{A}_i m(t) + \mathcal{A}_{di} m(t - d_1(t)) + \mathcal{B}_i u(t) + \mathcal{B}_{\omega i}\omega(t) + f(m,t) \\ z(t) & = & \mathcal{E}_i m(t) + \mathcal{E}_{di} m(t - d_1(t)) \\ y(t) & = & \mathcal{C}_i m(t) + \mathcal{C}_{di} m(t - d_1(t)) \\ m(t) & = & \tilde{\varphi}(t), \quad t \in [-\bar{d}_1, 0] \end{array} \tag{1}$$

where $m(t) \in \mathfrak{R}^m$ presents the state vector with $i = 1, 2, \cdots, \ell$, where ℓ denotes the number of **IF-THEN** rules; $u(t) \in \mathfrak{R}^n$ represents the control input vector; measured output is by $y(t) \in \mathfrak{R}^p$; and $\omega(t) \in \mathfrak{R}^q$ indicates the extraneous disturbance of the nonlinear model which is supposed to belong to $\mathcal{L}_2[0, \infty)$. $\bar{\vartheta}_j(t)(j = 1, 2, \cdots, g)$ and $\bar{W}_{ij}$ present the premise parameters and the fuzzy sets, respectively; $f(m,t)$ represents the known nonlinear continuous terms; $d_1(t)$ is the time-varying delay which fulfills $0 < d_1(t) \leq \bar{d}_1$ and $\dot{d}_1(t) \leq \mu_1$, where $\bar{d}_1$ and μ_1 were prescribed positive constants; Initial condition $\tilde{\varphi}(t)$ is defined over the domain $[-\bar{d}_1; 0]$. In this article, we suppose that $\bar{\vartheta}_j(t)$ is accessible. For simplicity, the authors present the term ∇_i instead of $\sum_{i=1}^{\ell} \bar{h}_i(\bar{\vartheta}(t))$. Using (1) as a starting point, we can then express the T-S fuzzy system as:

$$\begin{array}{rcl} \dot{m}(t) & = & \nabla_i\{\mathcal{A}_i m(t) + \mathcal{A}_{di} m(t - d_1(t)) + \mathcal{B}_i u(t) + \mathcal{B}_{\omega i}\omega(t)\} + f(m,t) \\ z(t) & = & \nabla_i\{\mathcal{E}_i m(t) + \mathcal{E}_{di} m(t - d_1(t))\} \\ y(t) & = & \nabla_i\{\mathcal{C}_i m(t) + + \mathcal{C}_{di} m(t - d_1(t))\} \\ m(t) & = & \tilde{\varphi}(t), \quad t \in [-\bar{d}_1, 0] \end{array} \tag{2}$$

where

$$\bar{h}_i(\bar{\vartheta}(t)) = \frac{\nu_i(\bar{\vartheta}(t))}{\sum_{i=1}^{\ell} \nu_i(\bar{\vartheta}(t))}, \quad \nu_i(\bar{\vartheta}(t)) = \prod_{j=1}^{g} \bar{W}_{ij}(\bar{\vartheta}(t)) \tag{3}$$

$\bar{W}_{ij}(\bar{\vartheta}_j(t)$ represents the membership degree of $\bar{\vartheta}_j(t)$ the fuzzy set $\bar{W}_{ij} \cdot \bar{h}_i(\bar{\vartheta}(t))$, which satisfies

$$\bar{h}_i(\bar{\vartheta}(t)) \geq 0, \quad \nabla_i = 1 \tag{4}$$

4 Formation of SMO

In this section, a two steps *SMO* design process is proposed for the *T-S fuzzy system*. The first step consists in constructing an *SMO* for system (2). In the second step, a novel sliding surface is designed for the new error system.

4.1 Construction of SMO

In this article, *SMO* will be considered as follows:

Fuzzy rule j : **IF** $\bar{\phi}(t)$ is $\bar{M}_{j1}$ and ... and $\bar{\phi}_g(t)$ is $\bar{M}_{jg}$, **THEN**

$$\begin{aligned} \dot{\hat{m}}(t) &= \mathcal{A}_j\hat{m}(t) + \mathcal{A}_{dj}\hat{m}(t-d_2(t)) + \mathcal{B}_j u(t) + \mathcal{L}_j(y(t)-\hat{y}(t)) + \mathcal{B}_j v(t) + f(\hat{m},t) \\ \hat{z}(t) &= \mathcal{E}_j\hat{m}(t) + \mathcal{E}_{dj}\hat{m}(t-d_2(t)) \\ \hat{y}(t) &= \mathcal{C}_j\hat{m}(t) + \mathcal{C}_{dj}\hat{m}(t-d_2(t)) \\ \hat{m}(t) &= \tilde{\varphi}_o(t), \quad t \in [-\bar{d}_2, 0] \end{aligned} \tag{5}$$

where $\hat{m}(t)$ presents the state estimation of $m(t)$, $\hat{y}(t)$ denotes the output to the observer, $\mathcal{L}_j \in \Re^{n\times p}$ are the *SMO* gain to be determined; $d_2(t)$ is the time-varying delay which fulfills $0 < d_2(t) \leq \bar{d}_2$ and $\dot{d}_2(t) \leq \mu_2$, where $\bar{d}_2$ and μ_2 were prescribed positive constants; $v(t)$ presents the nonlinear input; $\tilde{\phi}_o(t)$ is the initial function for the observer states. $\bar{\phi}_g(t)(g = 1, 2, \cdots, g)$ and $\bar{M}_{jg}$ are premise parameters and the fuzzy sets of observer–states, respectively. As a result of fuzzy blending, the overall *delayed T-S fuzzy SMO* system takes the following form:

$$\begin{aligned} \dot{\hat{m}}(t) &= \textstyle\sum_{i,j=1}^{\ell} \bar{h}_i(\bar{\phi}(t))\bar{h}_j(\bar{\phi}(t))\{\mathcal{A}_j\hat{m}(t) + \mathcal{A}_{dj}\hat{m}(t-d_2(t)) + \mathcal{B}_j u(t) + \mathcal{L}_j(y(t)-\hat{y}(t)) + \mathcal{B}_j v(t)\} + f(\hat{m},t) \\ \hat{z}(t) &= \textstyle\sum_{j=1}^{\ell} \bar{h}_j(\bar{\phi}(t))\{\mathcal{E}_j\hat{m}(t) + \mathcal{E}_{dj}\hat{m}(t-d_2(t))\} \\ \hat{y}(t) &= \textstyle\sum_{j=1}^{\ell} \bar{h}_j(\bar{\phi}(t))\{\mathcal{C}_j\hat{m}(t) + \mathcal{C}_{dj}\hat{m}(t-d_2(t))\} \\ \hat{m}(t) &= \tilde{\varphi}_o(t), \quad t \in [-\bar{d}_2, 0] \end{aligned} \tag{6}$$

Now, we define:

$$\tilde{m}(t) = m(t) - \hat{m}(t)$$

Therefore, an error system is obtained as follows:

$$\begin{aligned} \dot{\tilde{m}}(t) &= \textstyle\sum_{i,j=1}^{\ell} \bar{h}_i(\bar{\phi}(t))\bar{h}_j(\bar{\phi}(t))\{\varphi\hat{m}(t) + (\mathcal{A}_i - \mathcal{L}_j\mathcal{C}_i)\tilde{m}(t) + (\mathcal{A}_{di} - \mathcal{L}_j\mathcal{C}_{di})\hat{m}(t-d_1(t)) \\ &- (\mathcal{A}_{dj} - \mathcal{L}_j\mathcal{C}_{dj})\hat{m}(t-d_2(t)) + (\mathcal{A}_{di} - \mathcal{L}_j\mathcal{C}_{di})\tilde{m}(t-d_1(t)) + \mathcal{B}_{w_i}\omega(t) \\ &- \mathcal{B}_i v(t)\} + (f(m,t) - f(\hat{m},t)) \end{aligned} \tag{7}$$

where

$$\varphi = \mathcal{A}_i - \mathcal{A}_j - \mathcal{L}_j\mathcal{C}_i + \mathcal{L}_j\mathcal{C}_j$$

Remark 1 *It is commonly acknowledged that particular system parameters are subject to inevitable delays as a result of stochastic instability with the increasing complexity of real–time systems, especially in process engineering. In nonlinear systems, it is quite common for such perturbations of parameters to occur in a random manner due probably to random fluctuations of the network loads, random failures and repairs of the components, and sudden climate changes. In this case, the statistical properties (nonlinearities and time–varying delays) could be obtained through statistical analysis. A number of engineering applications, including networked control systems, digital control of chemical processes, and localization systems of mobile robots, rely largely on abrupt climate changes that cause stochastic parameters and time delay systems, whose probability distribution laws can be obtained through statistical tests.*

4.2 Error System with Sliding Surface Design

To create an error system from the Figure 1, an integral–type sliding surface is designed as follows:

$$s(t) = \bar{\mathcal{G}}\tilde{m}(t) + \bar{\mathcal{G}}\int_0^t \sum_{i=1}^{\ell} \bar{h}_i(\bar{\phi}(\alpha))(\mathcal{L}_i\mathcal{C}_i\tilde{m}(\alpha))d\alpha \tag{8}$$

where $\bar{\mathcal{G}} \in \Re^{m\times n}$ is a given matrix which fulfills the condition $det(\bar{\mathcal{G}}\mathcal{B}_i) \neq 0$ and $rank\begin{bmatrix} \bar{\mathcal{G}} \\ \mathcal{C}_i \end{bmatrix} = rank(\mathcal{C}_i)$.

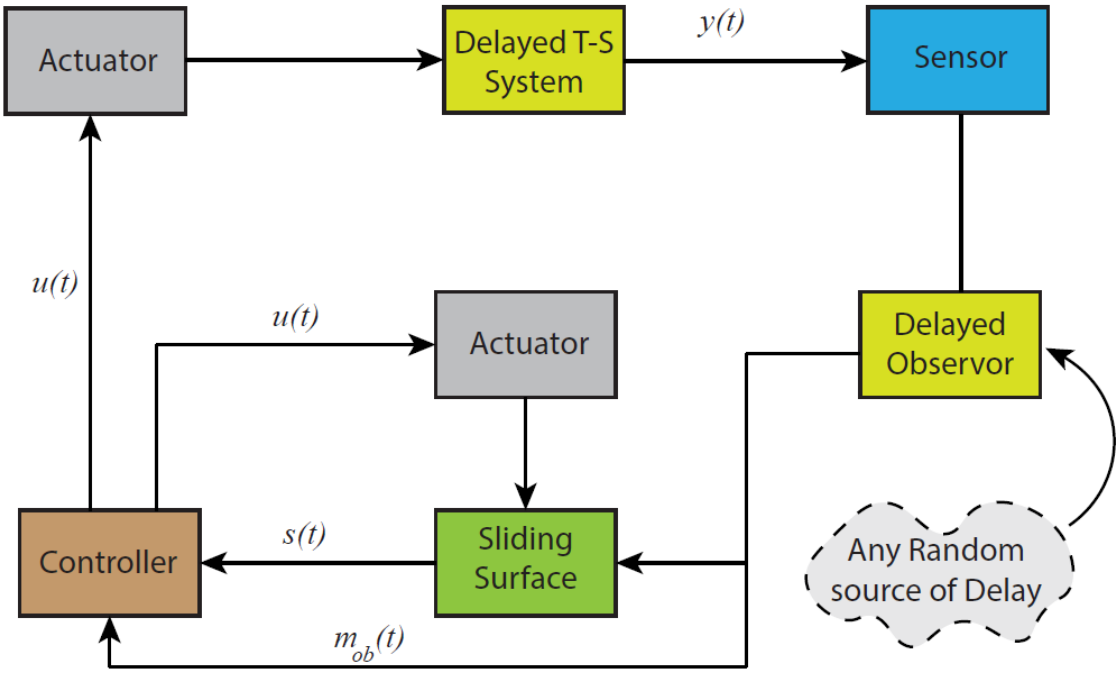

Figure 1: Observe-based sliding mode control.

Remark 2 *A fixed integrator setting keeps the system in its initial state on the sliding surface while ensuring fast response times and robustness. Moreover, to make calculation easier, we include* $\mathcal{L}_i\mathcal{C}_i\tilde{m}(t)$ *to* $s(t)$*. Based on these reasons, a universal flat surface is designed as (11).*

Remark 3 *This work adds a traditional integral sliding surface* $\bar{\mathcal{G}}\int_0^t\sum_{i=1}^{\ell}\bar{h}_i(\bar{\phi}(\alpha))(\mathcal{L}_i\mathcal{C}_i\tilde{m}(\alpha))d\alpha$*, to account for nonlinear functions. Literature [29] has extensively been applied in SMC research to inspire the choice of this integral sliding surface. With an integral sliding surface, the approach phase can be eliminated in the system's initial state so that the trajectory reaches the sliding surface, making the system globally robust and stable. The term* $s(t) = cm(t)$ *is a general formula for describing linear sliding surfaces. Practically,* m_0 *is never zero, i.e., its initial position is always uncertain. Nevertheless, integral sliding surfaces have the form* $s(t) = m(t) + cm(t)dt$*. Hence, if we set the integral* $\int m_0 dt = -\frac{m_0}{c}$ *for any initial state* m_0 *at any time, this enables us to guarantee that the sliding surface* $s(t) = 0$ *always results. Hence, ISMC is able to reduce chattering and steady–state errors better than conventional SMC.*

SMC theory asserts $s(t) = \dot{s}(t) = 0$, when sliding motion took place, we have

$$\begin{aligned}\dot{s}(t) &= \bar{\mathcal{G}}\sum_{i,j=1}^{\ell}\bar{h}_i(\bar{\phi}(t))h_j(\bar{\phi}(t))\{\varphi\hat{m}(t) + (\mathcal{A}_i - \mathcal{L}_j\mathcal{C}_i + \mathcal{L}_i\mathcal{C}_i)\tilde{m}(t)\\ &+ (\mathcal{A}_{di} - \mathcal{L}_j\mathcal{C}_{di})\hat{m}(t-d_1(t)) - (\mathcal{A}_{dj} - \mathcal{L}_j\mathcal{C}_{dj})\hat{m}(t-d_2(t))\\ &+ (\mathcal{A}_{di} - \mathcal{L}_j\mathcal{C}_{di})\tilde{m}(t-d_1(t)) + \mathcal{B}_{w_i}\omega(t)\\ &- \mathcal{B}_i v(t)\} + \bar{\mathcal{G}}\{(f(m,t) - f(\hat{m},t))\}\end{aligned} \tag{9}$$

Thus, from $\dot{s}(t) = 0$, we can obtain the following equivalent control law

$$\begin{aligned}v_{eq}(t) &= (\bar{\mathcal{G}}\mathcal{B}_j)^{-1}\bar{\mathcal{G}}(\sum_{i,j=1}^{\ell}\bar{h}_i(\bar{\phi}(t))\bar{h}_j(\bar{\phi}(t))\{\phi\hat{m}(t) + (\mathcal{A}_i - \mathcal{L}_j\mathcal{C}_i + \mathcal{L}_i\mathcal{C}_i)\tilde{m}(t)\\ &+ (\mathcal{A}_{di} - \mathcal{L}_j\mathcal{C}_{di})\hat{m}(t-d_1(t)) - (\mathcal{A}_{dj} - \mathcal{L}_j\mathcal{C}_{dj})\hat{m}(t-d_2(t))\\ &+ (\mathcal{A}_{di} - \mathcal{L}_j\mathcal{C}_{di})\tilde{m}(t-d_1(t)) + \mathcal{B}_{w_i}\omega(t)\} + (\bar{\mathcal{G}}\mathcal{B}_j)^{-1}\bar{\mathcal{G}}\{(f(m,t) - f(\hat{m},t))\}\end{aligned} \tag{10}$$

4.3 Construction of Sliding Surface for SMO System

In this section, we consider a new type of integral sliding function for the *T–S Fuzzy SMO* system (6).

$$s_1(t) = \bar{\mathcal{G}}_1\hat{m}(t) - \bar{\mathcal{G}}_1\int_0^t\sum_{i=1}^{\ell}\bar{h}_{i,j}(\bar{\phi}(\alpha))\{(\mathcal{A}_i+\mathcal{B}_i\mathcal{K}_j)\hat{m}(\alpha)+\mathcal{L}_i\mathcal{C}_i\hat{m}(\alpha)\}d\alpha \tag{11}$$

where $\bar{\mathcal{G}}_1 \in \Re^{m\times n}$ is a given matrix that fulfills the condition $det(\bar{\mathcal{G}}\mathcal{B}_i) \neq 0$ and $\mathcal{L}_i$ is defined in (6). On the other side, $\mathcal{K}_j$ is selected so that $(\mathcal{A}_i+\mathcal{B}_i\mathcal{K}_j)$ is Hurwitz. According to surface selected for sliding, the *SMC* theory asserts $s_1(t) = \dot{s}_1(t) = 0$, when sliding motion took place. In this scenario, the equivalent control law is designed as

$$\begin{aligned} u_{eq}(t) &= -(\bar{\mathcal{G}}_1\mathcal{B}_j)^{-1}\bar{\mathcal{G}}_1\sum_{i,j=1}^{\ell}\bar{h}_i(\bar{\phi}(t))\bar{h}_j(\bar{\phi}(t))\{(-\mathcal{B}_j\mathcal{K}_j+\mathcal{L}_i\mathcal{C}_i-\mathcal{L}_j\mathcal{C}_j+\mathcal{L}_j\mathcal{C}_i)\hat{m}(t) \\ &+ \mathcal{L}_i\mathcal{C}_i\tilde{m}(t)+\mathcal{L}_j\mathcal{C}_{di}\hat{m}(t-d_1(t))+(\mathcal{A}_{dj}-\mathcal{L}_j\mathcal{C}_{dj})\hat{m}(t-d_2(t)) \\ &+ \mathcal{L}_j\mathcal{C}_{di}\tilde{m}(t-d_1(t)-f(\hat{m},t)\}-v(t) \end{aligned} \tag{12}$$

In order to compute sliding mode dynamics, the equivalent control law comes from (12) shall be substituted into (7), with an estimate of the output error $e(t) = z(t) - \hat{z}(t)$ and vector that is augmented $\xi(t) = \begin{bmatrix}\hat{m}(t)\\ \tilde{m}(t)\end{bmatrix}$, then our augmented system becomes:

$$\begin{cases} \dot{\xi}(t) = \sum_{i,j,m=1}^{\ell}\bar{h}_i(\bar{\vartheta}(t))\bar{h}_j(\bar{\phi}(t))\hbar_m(\bar{\phi}(t))[\mathcal{A}_1\xi(t)+\sum_{\bar{k}=1}^{2}\mathcal{A}_{d_{\bar{k}}}\xi(t-d_{\bar{k}}(t))+\mathcal{B}_w\omega(t)]+(f(m,t)-f(\hat{m},t)) \\ e(t) = \sum_{i,j=1}^{\ell}\bar{h}_i(\bar{\vartheta}(t))\bar{h}_j(\bar{\phi}(t))[\mathcal{E}\xi(t)+\sum_{\bar{k}=1}^{2}\mathcal{E}_{d_{\bar{k}}}\xi(t-d_{\bar{k}}(t))] \end{cases} \tag{13}$$

where

$$\begin{aligned} \mathcal{A}_1 &= \begin{bmatrix}\varphi_a & -\varphi_1\mathcal{L}_i\mathcal{C}_i+\mathcal{L}_j\mathcal{C}_i \\ (I-\varphi_1)\varphi & (I-\varphi_1)(\mathcal{A}_i-\mathcal{L}_j\mathcal{C}_i+\mathcal{L}_i\mathcal{C}_i)\end{bmatrix}, \quad \mathcal{A}_{d_1} = \begin{bmatrix}\mathcal{L}_i\mathcal{C}_{di}-\varphi_1\mathcal{L}_j\mathcal{C}_{dj} & \mathcal{L}_i\mathcal{C}_{di}-\varphi_1\mathcal{L}_j\mathcal{C}_{di} \\ (I-\varphi_1)(\mathcal{A}_{di}-\mathcal{L}_j\mathcal{C}_{dj}) & (I-\varphi_1)(\mathcal{A}_{di}-\mathcal{L}_j\mathcal{C}_{di})\end{bmatrix} \\ \mathcal{A}_{d_2} &= \begin{bmatrix}\varphi_1(\mathcal{A}_{dj}-\mathcal{L}_j\mathcal{C}_{dj}) & 0 \\ -(I-\varphi_1)(\mathcal{A}_{dj}-\mathcal{L}_i\mathcal{C}_{dj}) & 0\end{bmatrix}, \quad \mathcal{B}_w = \begin{bmatrix}0 \\ (I-\varphi_1)\mathcal{B}_{w_i}\end{bmatrix}, \quad \varphi_1 = \mathcal{B}_i(\bar{\mathcal{G}}\mathcal{B}_i)^{-1}\bar{\mathcal{G}} \\ \varphi_a &= \mathcal{A}_j-\varphi_1(-\mathcal{B}_j\mathcal{K}_m+\mathcal{L}_i\mathcal{C}_i-\mathcal{L}_j\mathcal{C}_j), \quad \varphi = \mathcal{A}_i-\mathcal{A}_j-\mathcal{L}_j\mathcal{C}_i+\mathcal{L}_j\mathcal{C}_j \\ \mathcal{E} &= \begin{bmatrix}\mathcal{E}_i-\mathcal{E}_j & -\mathcal{E}_j\end{bmatrix}, \quad \mathcal{E}_{d_1} = \begin{bmatrix}\mathcal{E}_{di} & \mathcal{E}_{di}\end{bmatrix}, \quad \mathcal{E}_{d_2} = \begin{bmatrix}-\mathcal{E}_{dj} & 0\end{bmatrix} \end{aligned}$$

Remark 4 *It is well known that external disturbances can impact the stability of a system. Analyzing the system can lead to performance indicators, which can help determine its stability. For system analysis, the four standard single performances are commonly used: H_∞, passive, L_2-L_∞, and standard dissipative. Through the adjustment of weighting matrices and scalars, extended dissipative performances shall be converted into four common single performances that benefit systems analysis by providing as comprehensive and general a result as possible.*

Assumption 1 *In Lipschitz conditions, we assume that $g(m,t)$ is known and uniformly distributed over the states $m(t)$ and $\hat{m}(t)$, i.e.,*

$$\|g(m,t)-g(\hat{m},t)\| \leq \mathbb{L}_f \parallel m-\hat{m} \parallel, \forall \quad m,\hat{m} \in \Re^m$$

where $\mathbb{L}_f$ is known as a Lipschitz constant.

Lemma 1 **([46])** *Let's assume a matrix $\mathcal{C}_i \in \Re^{m\times n}$ of $rank(\mathcal{C}_i) = m$, the single value decomposition (SVD) for $\mathcal{C}_i$ can be presented in $\mathcal{C}_i = \mathbb{O}\begin{bmatrix}\mathbb{S} & 0\end{bmatrix}\mathbb{V}^t$, suppose $\mathcal{X}_i > 0$, $\mathbb{M} \in \mathcal{R}^{m\times m}$. Then, there exists $\bar{\mathcal{X}}_i$ such that $\mathcal{C}_i\mathcal{X}_i = \bar{\mathcal{X}}_i\mathcal{C}_i$, if and only if*

$$\mathcal{X}_i = \mathbb{V} * diag\{\mathbb{M},\mathbb{N}\} * \mathbb{V}^T$$

Theorem 1 *With the Definition [2, [47]] of dissipative property, let's consider the nonlinear system (13) with given $0 < O_g < 1$, and $\sum_{g=1}^{3} O_g = 1$, $\bar{d}_{\bar{k}}$, and γ, the closed–loop system (13) is extended dissipative for any time-varying delay $d_{\bar{k}}(t)$, which fulfills the equation $0 \leq d_{\bar{k}}(t) \leq \bar{d}_{\bar{k}}$, $\dot{d}_{\bar{k}}(t) \leq \mu_{\bar{k}}$. If matrices $\mathcal{P}_i > 0$, $\mathcal{S}_{\bar{k}} > 0$, $\mathcal{Q}_{\bar{k}i} > 0$, $\mathcal{R}_{\bar{k}i} > 0$, $\mathcal{Z}_{\bar{k}i} > 0$, $\mathcal{W}_\ell > 0$, $\mathcal{M}_{\bar{k}i}$ such that $(G-\mathcal{P}_i) < 0$, $\digamma_a := (\dot{\mathcal{Q}}_{\bar{k}i}+\dot{\mathcal{R}}_{\bar{k}i}-\mathcal{S}_{\bar{k}}) < 0$, $\digamma_b := (\dot{\mathcal{R}}_{\bar{k}i}-\mathcal{S}_{\bar{k}}) < 0$,*

$\digamma_c := (\dot{\mathcal{Z}}_{\bar{k}i} - \bar{d}_{\bar{k}}^{-1}\mathcal{W}_{\bar{k}}) < 0$, $\begin{bmatrix} \mathcal{Z}_{\bar{k}i} & -\mathcal{M}_{\bar{k}i} \\ (\bullet) & \mathcal{Z}_{\bar{k}i} \end{bmatrix} > 0$, $i = 1, 2, \cdots, \ell$, $\bar{k} = 1, 2$, *then the inequalities stated below apply.*

$$\triangle_{ij} = \begin{bmatrix} \triangle_{ij}^{11} & \triangle_{ij}^{12} \\ (\bullet) & -I \end{bmatrix} < 0, \tag{14}$$

$$\prod_{ij} = \begin{bmatrix} \prod_{ij}^{11} & \prod_{ij}^{12^T} & \prod_{ij}^{13^T} & \prod_{ij}^{14^T} & \mathcal{P}_i \\ (\bullet) & -\Gamma_3 & \mathcal{B}_\omega^T\mathcal{P}_i & 0 & 0 \\ (\bullet) & (\bullet) & \mathbb{Z}_i - 2\mathcal{P}_i & 0 & 0 \\ (\bullet) & (\bullet) & (\bullet) & -I & 0 \\ (\bullet) & (\bullet) & (\bullet) & 0 & -kI \end{bmatrix} < 0 \tag{15}$$

where

$$\prod_{ij}^{11} = \begin{bmatrix} \Pi_{ij}^{11} & \mathcal{P}_i\mathcal{A}_{d_1} & \mathcal{M}_{1i} & \mathcal{P}_iA_{d_2} & \mathcal{M}_{2i} \\ (\bullet) & \partial_{1i} & 0 & 0 & 0 \\ (\bullet) & (\bullet) & \partial_{3i} & 0 & 0 \\ (\bullet) & (\bullet) & (\bullet) & \partial_{2i} & 0 \\ (\bullet) & (\bullet) & (\bullet) & (\bullet) & \partial_{4i} \end{bmatrix}$$

$$\triangle_{ij}^{11} = diag\{-O_1G, -O_2G, -O_3G\}, \quad \triangle_{ij}^{12} = col\{\mathcal{E}^T\tilde{\Gamma}_0, \mathcal{E}_{d_1}^T\tilde{\Gamma}_0, \mathcal{E}_{d_2}^T\tilde{\Gamma}_0\}$$

$$\Pi_{ij}^{11} = \dot{\mathcal{P}}_i + \mathcal{P}_i\mathcal{A}_1 + \mathcal{A}_1^T\mathcal{P}_i + \sum_{\bar{k}=1}^{2}\left(\mathcal{Q}_{\bar{k}i} + \mathcal{R}_{\bar{k}i} - \mathcal{Z}_{\bar{k}i} + \bar{d}_{\bar{k}}\mathcal{S}_{\bar{k}}\right) + aI$$

$$\prod_{ij}^{12} = \begin{bmatrix} -\Gamma_2^T\mathcal{E} + \mathcal{B}_w^T\mathcal{P}_i & -\Gamma_2^T\mathcal{E}_{d_1} & 0 & -\Gamma_2^T\mathcal{E}_{d_2} & 0 \end{bmatrix}$$

$$\prod_{ij}^{13} = \begin{bmatrix} \mathcal{P}_i\mathcal{A}_1 & \mathcal{P}_i\mathcal{A}_{d_1} & 0 & \mathcal{P}_i\mathcal{A}_{d_2} & 0 \end{bmatrix}$$

$$\prod_{ij}^{14} = \begin{bmatrix} \tilde{\Gamma}_1\mathcal{E} & \tilde{\Gamma}_1\mathcal{E}_{d_1} & 0 & \tilde{\Gamma}_1\mathcal{E}_{d_2} & 0 \end{bmatrix}$$

$$\mathbb{Z}_i = \sum_{\bar{k}=1}^{2}\left(\mathcal{Z}_{\bar{k}i} + 1/2\bar{d}_{\bar{k}}^2\mathcal{W}_{\bar{k}}\right), \quad a = k\mathbb{L}_f$$

$$\partial_{\bar{k}i} = -(1-\mu_{\bar{k}})\mathcal{Q}_{\bar{k}i}, \quad \partial_{2+\bar{k}i} = -\mathcal{R}_{\bar{k}i} - \mathcal{Z}_{\bar{k}i}, \quad \bar{k} = 1, 2.$$

Remark 5 *According to Theorem 1, a stable sliding motion takes place on the infinite-time sliding surface using the control law $u(t)$ defined in (12) and (11). According to equation (16), the fuzzy Lyapunov candidate function is defined after the sliding surface has reached the states on the sliding surface defined in equation (11). The asymptotic stability of the sliding surface is determined by the derivative of the mode-dependent fuzzy Lyapunov function in equation (20). Throughout the slide, the states are clearly shown to remain on the sliding surface. Additionally, if a sliding surface is defined, it will converge within a limited time period.*

Proof. In this stage, the Krasovskii–Lyapunov function for system (13) is implemented as

$$\mathcal{T}(m_t, t) = \xi(t)^T\mathcal{P}_i\xi(t) + \sum_{\bar{g}=1}^{3}\mathcal{T}_{\bar{g}}(t) \tag{16}$$

where

$$\mathcal{T}_1(t) = \sum_{\bar{k}=1}^{2}\left(\int_{t-d_{\bar{k}}(t)}^{t}\xi(v)^T\mathcal{Q}_{\bar{k}i}\xi(v)dv + \int_{t-\bar{d}_{\bar{k}}}^{t}\zeta(v)^T\mathcal{R}_{\bar{k}i}\zeta(v)\right)dv$$

$$\mathcal{T}_2(t) = \sum_{\bar{k}=1}^{2}\left(\bar{d}_{\bar{k}}\int_{-\bar{d}_{\bar{k}}}^{0}\int_{t+\beta}^{t}\dot{\xi}(v)^T\mathcal{Z}_{\bar{k}i}\dot{\xi}(v)dvd\beta + \int_{-\bar{d}_{\bar{k}}}^{0}\int_{t+\beta}^{t}\xi(v)^T\mathcal{S}_{\bar{k}}\xi(v)\right)dvd\beta$$

$$\mathcal{T}_3(t) \;=\; \sum_{\bar{k}=1}^{2}\left(\int_{-\bar{d}_{\bar{k}}}^{0}\int_{\theta}^{0}\int_{t+\beta}^{t}\dot{\xi}(\upsilon)^T\mathcal{W}_{\bar{k}}\dot{\xi}(\upsilon)\right)d\upsilon d\beta d\theta$$

From the above-mentioned Lyapunov function, we have $\mathcal{P}_i > 0$, $\mathcal{Q}_{\bar{k}i} > 0$, $\mathcal{R}_{\bar{k}i} > 0$, $\mathcal{Z}_{\bar{k}i} > 0$, $\mathcal{S}_{\bar{k}} > 0$, and $\mathcal{W}_{\bar{k}} > 0$. Then, computing the derivative of $\mathcal{T}_{\bar{g}}(t)$ $(\bar{g} = 1, 2, 3)$ along with the system (13), we have:

$$\begin{aligned}
\dot{\mathcal{T}}(m_t,t) \;\leq\; & \xi(t)^T(\dot{\mathcal{P}}_i + \sum_{\bar{k}=1}^{2}(\mathcal{Q}_{\bar{k}i} + \mathcal{R}_{\bar{k}i} + \bar{d}_{\bar{k}}\mathcal{S}_{\bar{k}}))\zeta(t) + 2\xi(t)^T\mathcal{P}_i\dot{\xi}(t) \\
& - \sum_{\bar{k}=1}^{2}(1-\dot{d}_{\bar{k}}(t))\xi(t-d_{\bar{k}}(t))^T\mathcal{Q}_{\bar{k}i}\xi(t-d_{\bar{k}}(t)) \\
& - \sum_{\bar{k}=1}^{2}\left(\xi(t-\bar{d}_{\bar{k}})^T\mathcal{R}_{\bar{k}i}\xi(t-\bar{d}_{\bar{k}}) - \dot{\xi}(t)^T\left(\bar{d}_{\bar{k}}^2\mathcal{Z}_{\bar{k}i} + 1/2d_{\bar{k}}^2\mathcal{W}_{\bar{k}}\right)\right)\dot{\xi}(t) \\
& - \sum_{\bar{k}=1}^{2}\bar{d}_{\bar{k}}\int_{t-\bar{d}_{\bar{k}}}^{t}\dot{\xi}(\upsilon)^T\mathcal{Z}_{\bar{k}i}\dot{\xi}(\upsilon)d\upsilon + 2\xi(t)^T\mathcal{P}_i\left[f(m,t) - f(\hat{m},t)\right] \\
& + \sum_{\bar{k}=1}^{2}\int_{t-d_{\bar{k}}(t)}^{t}\xi(\upsilon)^T\mathcal{F}_a\xi(\upsilon)d\upsilon + \sum_{\bar{k}=1}^{2}\int_{t-\bar{d}_{\bar{k}}}^{t-d_{\bar{k}}(t)}\xi(\upsilon)^T\mathcal{F}_b\xi(\upsilon)d\upsilon \\
& + \sum_{\bar{k}=1}^{2}\bar{d}_{\bar{k}}\int_{-\bar{d}_{\bar{k}}}^{0}\int_{t+\beta}^{t}\dot{\xi}(\upsilon)^T\mathcal{F}_c\dot{\xi}(\upsilon)d\upsilon d\beta
\end{aligned} \tag{17}$$

Because the inequality $2A^TB \leq \frac{1}{k}A^TA + kB^TB$ is valid for any integer $k > 0$, we notice that:

$$\sum_{\bar{k}=1}^{2}\bar{d}_{\bar{k}}\int_{t-\bar{d}_{\bar{k}}}^{t}\dot{\xi}(\upsilon)^T\mathcal{Z}_{\bar{k}i}\dot{\xi}(\upsilon)d\upsilon \geq \begin{bmatrix}\xi(t)\\ \xi(t-\bar{d}_{\bar{k}})\end{bmatrix}^T\begin{bmatrix}\mathcal{Z}_{\bar{k}i} & -\mathcal{M}_{\bar{k}i}\\ (\bullet) & \mathcal{Z}_{\bar{k}i}\end{bmatrix}\begin{bmatrix}\xi(t)\\ \xi(t-\bar{d}_{\bar{k}})\end{bmatrix} \tag{18}$$

The definition of the augmented matrix follows

$$\eta(t) = col[\xi(t), \xi(t-d_1(t)), \xi(t-\bar{d}_1), \xi(t-d_2(t)), \xi(t-\bar{d}_2), \omega(t)]$$

Combining (17) and (18), we get

$$\dot{\mathcal{T}}(m_t,t) - \mathbb{J}(t) \;\leq\; \eta^T(t)\prod_{ij}\eta(t)$$

Let us consider

$$\mathbb{Z}_i = \mathcal{P}_i[\mathcal{P}_i\mathbb{Z}_i^{-1}\mathcal{P}_i]\mathcal{P}_i \leq \mathcal{P}_i[2\mathcal{P}_i - \mathbb{Z}_i]^{-1}\mathcal{P}_i$$

From this, it follows that

$$\prod_{ij} \;\leq\; \begin{bmatrix}\Pi_{ij}^{11} & \Pi_{ij}^{12^T}\\ (\bullet) & -\Gamma_3\end{bmatrix} + \begin{bmatrix}\Pi_{ij}^{13^T}\\ \mathcal{B}_w^T\end{bmatrix}\mathcal{P}_i[2\mathcal{P}_i - \mathbb{Z}_i]^{-1}\mathcal{P}_i\begin{bmatrix}\Pi_{ij}^{13^T}\\ \mathcal{B}_w^T\end{bmatrix}^T + \begin{bmatrix}\Pi_{ij}^{14^T}\\ 0\end{bmatrix}\tilde{\Gamma}_1^T\tilde{\Gamma}_1\begin{bmatrix}\Pi_{ij}^{14^T}\\ 0\end{bmatrix}^T \tag{19}$$

Then, by applying the Schur complement, we obtain (14). Thus, the matrix on *RHS* (19) is non-positive certain, and therefore $\prod_{ij} < 0$ is valid. The result of this is that, given by (17)–(18).

$$\dot{\mathcal{T}}(m_t,t) - \mathbb{J}(t) \leq 0 \tag{20}$$

As a result, the following proof of [[45], Theorem 1] will follow the same procedure. In the same consequences, it is not problematic to get the fault system (13) to be stretched dissipative, according to the Definition [2, [47]]. As a result, the proof can be concluded readily. □

By applying *Theorem 1* to *Theorem 2*, now we are in a situation to design an observer and controller for the forms (13).

Theorem 2 *With the Definition [2, [47]] of dissipative phenomena, let's consider the nonlinear system (13) to the given $0 < O_g < 1$, and $\sum_{g=1}^{3} O_g = 1$, $\bar{d}_{\bar{k}}$, and γ under the closed-loop system (13) is extended dissipative for any time-varying delays $d_{\bar{k}}(t)$, which fulfills the equation $0 \leq d_{\bar{k}}(t) \leq \bar{d}_{\bar{k}}$, $\dot{d}_{\bar{k}}(t) \leq \mu_{\bar{k}}$. If matrices $\bar{\mathcal{P}}_i > 0$, $\bar{\mathcal{S}}_{\bar{k}} > 0$, $\mathcal{X}_i > 0$, $\bar{\mathcal{Q}}_{\bar{k}i} > 0$, $\bar{\mathcal{R}}_{\bar{k}i} > 0$, $\bar{\mathcal{Z}}_{\bar{k}i} > 0$, $\bar{\mathcal{W}}_\ell > 0$, $\bar{\mathcal{M}}_{\bar{k}i}$ such that $i = 1, 2, \cdots, \ell$, $\bar{k} = 1, 2$, then the below inequalities hold:*

$$\bar{\triangle}_{ij} + \bar{\triangle}_{ji} < 0, \quad i \leq j \tag{21}$$

$$\bar{\prod}_{ij} + \bar{\prod}_{ji} < 0, \quad i \leq j \tag{22}$$

$$\begin{cases} \sum_{i=1}^{\ell} \rho_i [\bar{\mathcal{Q}}_{\bar{k}i} + \bar{\mathcal{R}}_{\bar{k}i} + \mathcal{L}_{\bar{k}}] - \bar{\mathcal{S}}_{\bar{k}} < 0 \\ \bar{\mathcal{Q}}_{\bar{k}i} + \bar{\mathcal{R}}_{\bar{k}i} + \mathcal{L}_{\bar{k}} > 0 \end{cases} \tag{23}$$

$$\begin{cases} \sum_{i=1}^{\ell} \rho_i [\bar{\mathcal{R}}_{\bar{k}i} + \bar{\mathcal{K}}_{\bar{k}}] - \bar{\mathcal{S}}_{\bar{k}} < 0 \\ \bar{\mathcal{R}}_{\bar{k}i} + \bar{\mathcal{K}}_{\bar{k}} > 0 \end{cases} \tag{24}$$

$$\begin{cases} \sum_{i=1}^{\ell} \rho_i [\bar{\mathcal{Z}}_{\bar{k}i} + \bar{\mathcal{N}}_{\bar{k}}] - \frac{1}{\bar{d}_{\bar{k}}} \bar{\mathcal{W}}_{\bar{k}} < 0 \\ \bar{\mathcal{Z}}_{\bar{k}i} + \bar{\mathcal{N}}_{\bar{k}} > 0 \end{cases} \tag{25}$$

$$\bar{G} - \mathcal{X} < 0, \ \begin{bmatrix} \bar{\mathcal{Z}}_{\bar{k}i} & -\bar{\mathcal{M}}_{\bar{k}i} \\ (\bullet) & \bar{\mathcal{Z}}_{\bar{k}i} \end{bmatrix} > 0, \ (\mathcal{X}_i + \mathcal{L}_0) > 0 \tag{26}$$

where

$$\bar{\triangle}_{ij} = \begin{bmatrix} -O_1 \bar{G} & 0 & 0 & \top_{1ij} \tilde{\Gamma}_0 \\ (\bullet) & -O_2 \bar{G} & 0 & \top_{2ij} \tilde{\Gamma}_0 \\ (\bullet) & (\bullet) & -O_3 \bar{G} & \top_{3ij} \tilde{\Gamma}_0 \\ (\bullet) & (\bullet) & (\bullet) & -I \end{bmatrix}$$

$$\bar{\prod}_{ij}^{11} = \begin{bmatrix} \bar{\Pi}_{ij}^{11} & \exists_{2ij} & \bar{\mathcal{M}}_{1i} & \exists_{3ij} & \bar{\mathcal{M}}_{2i} & \beth_{ij} & \exists_{1ij}^T & \top_1 \tilde{\Gamma}_1 & \mathcal{X}_i \\ (\bullet) & \bar{\partial}_{1i} & 0 & 0 & 0 & -\top_2 \Gamma_2 & \exists_{2ij}^T & \top_2 \tilde{\Gamma}_1 & 0 \\ (\bullet) & (\bullet) & \bar{\partial}_{3i} & 0 & 0 & 0 & 0 & 0 & 0 \\ (\bullet) & (\bullet) & (\bullet) & \bar{\partial}_{2i} & 0 & -\top_3 \Gamma_2 & \exists_{3ij}^T & \top_3 \tilde{\Gamma}_1 & 0 \\ (\bullet) & (\bullet) & (\bullet) & (\bullet) & \bar{\partial}_{4i} & 0 & 0 & 0 & 0 \\ (\bullet) & (\bullet) & (\bullet) & (\bullet) & (\bullet) & -\Gamma_3 I & \mathcal{B}_\omega^T & 0 & 0 \\ (\bullet) & (\bullet) & (\bullet) & (\bullet) & (\bullet) & (\bullet) & \bar{\mathbb{Z}}_i - 2\bar{\mathcal{P}}_i & 0 & 0 \\ (\bullet) & (\bullet) & (\bullet) & (\bullet) & (\bullet) & (\bullet) & (\bullet) & -I & 0 \\ (\bullet) & (\bullet) & (\bullet) & (\bullet) & (\bullet) & (\bullet) & (\bullet) & (\bullet) & -kI \end{bmatrix}$$

$$\bar{\Pi}_{ij}^{11} = \sum_{i=1}^{\ell} \{ \begin{bmatrix} I \\ 0 \end{bmatrix} \rho_i (\mathcal{X}_i + \mathcal{L}_0) \begin{bmatrix} I & 0 \end{bmatrix} \} + \exists_{1ij} + \exists_{1ij}^T + \sum_{\bar{k}=1}^{2} \left(\bar{\mathcal{Q}}_{\bar{k}i} + \bar{\mathcal{R}}_{\bar{k}i} - \bar{\mathcal{Z}}_{\bar{k}i} + \bar{d}_{\bar{k}} \bar{\mathcal{S}}_{\bar{k}} \right)$$

$$\bar{\mathbb{Z}}_i = \sum_{\bar{k}=1}^{2} \left(\bar{\mathcal{Z}}_{\bar{k}i} + 1/2 \bar{d}_{\bar{k}}^2 \bar{\mathcal{W}}_{\bar{k}} \right), \quad \bar{\partial}_{\bar{k}i} = -(1 - \mu_{\bar{k}}) \bar{\mathcal{Q}}_{\bar{k}i}$$

$$\bar{\partial}_{(2+\bar{k})i} = -\bar{\mathcal{R}}_{\bar{k}i} - \bar{\mathcal{Z}}_{\bar{k}i}, \ \bar{k} = 1, 2. \quad \beth_{ij} = \mathcal{B}_\omega - \top_1 \Gamma_2$$

$$\exists_{1ij} = \begin{bmatrix} \Omega_1^a + \varphi_1 \Omega_1^b & \varphi_1 \mathcal{A}_i \mathcal{X}_j - \varphi_1 \mathcal{F}_j \mathcal{C}_j \\ (I - \varphi_1) \Omega_1^b & (I - \varphi_1)(\mathcal{A}_i \mathcal{X}_j - \mathcal{F}_j \mathcal{C}_j) \end{bmatrix}$$

$$\exists_{2ij} = \begin{bmatrix} \varphi_1 \mathcal{A}_{di} \mathcal{X}_j + \mathcal{F}_j \mathcal{C}_{dj} + \varphi_1 \mathcal{F}_j \mathcal{C}_{dj} & \varphi_1 \mathcal{A}_{di} \mathcal{X}_j + \mathcal{F}_j \mathcal{C}_{di} + \varphi_1 \mathcal{F}_j \mathcal{C}_{dj} \\ (I - \varphi_1)(\mathcal{A}_{dj} \mathcal{X}_j + \mathcal{F}_j \mathcal{C}_{di}) & (I - \varphi_1)(\mathcal{A}_{di} \mathcal{X}_j + \mathcal{F}_j \mathcal{C}_{di}) \end{bmatrix}$$

$$
\begin{aligned}
\exists_{3ij} &= \begin{bmatrix} \varphi_1(\mathcal{A}_{dj}\mathcal{X}_j - \mathcal{F}_j\mathcal{C}_{dj}) & 0 \\ -(I-\varphi_1)(\mathcal{A}_{dj}\mathcal{X}_j - \mathcal{F}_j\mathcal{C}_{dj}) & 0 \end{bmatrix}, \quad \top_{1ij} = 1_2 \otimes (\mathcal{X}_j(\mathcal{E}_i^T - \mathcal{E}_j^T)) \\
\top_{2ij} &= 1_2 \otimes (\mathcal{X}_j\mathcal{E}_{di}^T), \quad \top_{3ij} = \begin{bmatrix} -\mathcal{X}_j\mathcal{E}_{di}^T \\ 0 \end{bmatrix} \\
\Omega_1^a &= \mathcal{A}_j\mathcal{X}_j - \varphi_1(-\mathcal{B}_j\mathcal{Y}_m + \mathcal{F}_j\mathcal{C}_i - \mathcal{F}_j\mathcal{C}_j), \quad \Omega_1^b = (\mathcal{A}_i - \mathcal{A}_j)\mathcal{X}_j - \mathcal{F}_j\mathcal{C}_i - \mathcal{F}_j\mathcal{C}_j
\end{aligned}
$$

The following are the gains for controllers and observers:

$$
\mathcal{K}_m = \mathcal{Y}_j\mathcal{X}_i^{-1}, \qquad \mathcal{L}_j = \mathcal{F}_j\mathbb{O}\mathbb{S}\mathcal{X}_i^{-1}\mathbb{S}^{-1}\mathbb{O}^{-1} \tag{27}
$$

Proof. First, we define:

$$
\mathcal{P}_i = diag\{\bar{\mathcal{P}}_i, \bar{\mathcal{P}}_i\} \tag{28}
$$

$\mathcal{X}_i = \bar{\mathcal{P}}_i^{-1}$, $\mathcal{X}_i\mathcal{Q}_{\bar{k}i}\mathcal{X}_i = \bar{\mathcal{Q}}_{\bar{k}i}$, $\mathcal{X}_i\mathcal{R}_{\bar{k}i}\mathcal{X}_i = \bar{\mathcal{R}}_{\bar{k}i}$, $\mathcal{X}_i\mathcal{Z}_{\bar{k}i}\mathcal{X}_i = \bar{\mathcal{Z}}_{\bar{k}i}$, $\mathcal{X}_i\mathcal{M}_{\bar{k}i}\mathcal{X}_i = \bar{\mathcal{M}}_{\bar{k}i}$, $\mathcal{X}_i\mathcal{P}_i\mathcal{X}_i = \bar{\mathcal{P}}_i$
For $\mathcal{X}_i = \mathcal{V}\,(diag\{\mathcal{X}_{1i}, \mathcal{X}_{2i}\})\,\mathcal{V}^T$. According to Lemma 1, with the assumption $\mathcal{C}_i\mathcal{X}_i = \bar{\mathcal{X}}_i\mathcal{C}_i$ where $\bar{\mathcal{X}}_i^{-1} = \mathbb{O}\mathbb{S}\mathcal{X}_{1i}^{-1}\mathbb{S}^{-1}\mathbb{O}^{-1}$. Find (14), then pre- and post–multiply by $\{\mathcal{X}_i, \mathcal{X}_i, \mathcal{X}_i, I\}$ and their transpose leads to (21). Accordingly, pre- and post–multiply to (15) by $\{\underbrace{\mathcal{X}_i, \cdots, \mathcal{X}_i}_{5}, I, \mathcal{X}_i, I, \mathcal{X}_i\}$ and its transpose, yields (22).

Then, we define: $\bar{\mathcal{X}}_i = \sum_{i=1}^{\ell}\hbar_i\bar{\mathcal{X}}_i$, $\bar{\mathcal{R}}_{\bar{k}i} = \sum_{i=1}^{\ell}\hbar_i\bar{\mathcal{R}}_{\bar{k}i}$, $\bar{\mathcal{Q}}_{\bar{k}i} = \sum_{i=1}^{\ell}\hbar_i\bar{\mathcal{Q}}_{\bar{k}i}$, $\bar{\mathcal{M}}_{\bar{k}i} = \sum_{i=1}^{\ell}\hbar_i\bar{\mathcal{M}}_{\bar{k}i}$, and $\bar{\mathcal{Z}}_{\bar{k}i} = \sum_{i=1}^{\ell}\hbar_i\bar{\mathcal{Z}}_{\bar{k}i}$.

As a result, it can be demonstrated that

$$
\bar{\mathcal{X}}_i > 0,\ \bar{\mathcal{R}}_{\bar{k}i} > 0,\ \bar{\mathcal{Q}}_{\bar{k}i} > 0,\ \bar{\mathcal{Z}}_{\bar{k}i} > 0,\ \bar{G} - \bar{\mathcal{P}}_i < 0, \quad \begin{bmatrix} \bar{\mathcal{Z}}_{\bar{k}i} & -\bar{\mathcal{M}}_{\bar{k}i} \\ (\bullet) & \bar{\mathcal{Z}}_{\bar{k}i} \end{bmatrix} > 0.
$$

It is important to note the following equality

$$
\sum_{i=1}^{\ell}\bar{\hbar}_i = 1, \qquad \Rightarrow \sum_{i=1}^{\ell}\dot{\bar{\hbar}}_i = 0
$$

In this, we suppose the assumption with constant positive number ρ_i exists, such that

$$
\dot{\bar{\hbar}}_i \le \rho_i, \quad i = 1, 2, 3, \cdots, \ell \tag{29}
$$

This assumption is with the condition $(\mathcal{X}_i + \mathcal{L}_0) > 0$ which is established in (26). Thus, we get the following result:

$$
\dot{\mathcal{X}}_i = \sum_{i=1}^{\ell}\dot{\bar{\hbar}}_i\mathcal{X}_i = \sum_{i=1}^{\ell}\dot{\bar{\hbar}}_i(\mathcal{X}_i + \mathcal{L}_0) \le \sum_{i=1}^{\ell}\rho_i(\mathcal{X}_i + \mathcal{L}_0)
$$

Suppose

$$
\dot{\bar{\hbar}}_i \le \rho_i \qquad \Rightarrow \dot{\bar{\hbar}}_i \le \rho_i \quad \Rightarrow \rho_i > 0, \quad \Rightarrow \sum_{i=1}^{\ell}\dot{\bar{\hbar}}_i = 0
$$

$$
\begin{aligned}
\dot{\mathcal{X}}_i &= \sum_{i=1}^{\ell}\dot{\bar{\hbar}}_i\mathcal{X}_i, \quad = \sum_{i=1}^{\ell}\dot{\bar{\hbar}}_i(\mathcal{X}_i + \mathcal{L}_0), \\
&\le \sum_{i=1}^{\ell}\rho_i\underbrace{(\mathcal{X}_i + \mathcal{L}_0)}_{>0}
\end{aligned}
$$

With the additional computations combined with (22), this implies

$$
\bar{\prod}_{ij} < 0
$$

In (22), the inequality was satisfied. On the other hand, we can confirm that condition (14) is fulfilled when (21) holds. Accordingly, we proved the condition with the assumption for a constant positive number ρ_i exist, which

yields to the eq. (23) by adopting the same process of [41]. In addition, the same mathematical step will be adopted for the remaining inequalities in (24)-(25), which implies that

$$(\dot{\mathcal{R}}_{\bar{k}i} - \mathcal{S}_{\bar{k}}) < 0, \qquad (\dot{\mathcal{Z}}_{\bar{k}i} - \bar{d}_{\bar{k}}^{-1}\mathcal{W}_{\bar{k}}) \tag{30}$$

Therefore, all conditions in *Theorem 2* are satisfied while the given *LMIs* (21)-(26) are viable. The proof could be prepared subsequently. □

5 Construction of SMC

In this subsection, the *SMO* and error control systems are described using sliding mode controllers.

5.1 Error system controller with sliding mode

First, if the *LMIs* in Theorem 2 are feasible, then it implies that $\tilde{m}(t)$ is bounded. We assume that $\|\tilde{m}(t)\| \leq \kappa$ where κ is known as a positive constant.

Corollary 1 *With the proper dimension of $\bar{\mathcal{G}}$, the sliding mode motion can be obtained for the sliding surface $s(t) = 0$ by the following* SMC *law.*

$$\begin{aligned} v(t) &= (\bar{\mathcal{G}}\mathcal{B}_j)^{-1}\Big(\sum_{i,j=1}^{\ell} \bar{\hbar}_i(\bar{\phi}(t))\bar{\hbar}_j(\bar{\phi}(t)) + \{\bar{\mathcal{G}}(\mathcal{A}_i - \mathcal{L}_j\mathcal{C}_i + \mathcal{L}_i\mathcal{C}_i)\tilde{m}(t) \\ &+ \bar{\mathcal{G}}(\mathcal{A}_{di} - \mathcal{L}_j\mathcal{C}_{di})\tilde{m}(t - d_1(t))\} + \delta_i \frac{s(t)}{\| s(t) \|} \end{aligned} \tag{31}$$

where

$$\delta_i = (\| \bar{\mathcal{G}}\mathcal{A}_i \| + \| \bar{\mathcal{G}}(\mathcal{A}_{di} - \mathcal{L}_j\mathcal{C}_{di}) \|) - \| \bar{\mathcal{G}}(\mathcal{A}_{dj} - \mathcal{L}_j\mathcal{C}_{dj}) \|)\kappa + \| \bar{\mathcal{G}}\mathcal{B}_{\omega i} \| \theta + \bar{\mathcal{G}}\mathbb{L}_f + \delta_0$$

with θ as disturbance bounded and δ_0 as a positive scalar.

Proof. In this stage, we select the following Lyapunov function

$$\mathcal{T}_a(m_t, t) = \frac{1}{2}s(t)^T s(t)$$

Computing the time–derivative of $\mathcal{T}_a(m_t, t)$, we get:

$$\begin{aligned} \dot{\mathcal{T}}_a(m_t, t) &= s(t)^T \dot{s}(t) \\ &= s(t)^T \{\bar{\mathcal{G}} \sum_{i,j=1}^{\ell} \bar{\hbar}_i(\bar{\phi}(t))\hbar_j(\bar{\phi}(t))\{\varphi\hat{m}(t) + (\mathcal{A}_i - \mathcal{L}_j\mathcal{C}_i + \mathcal{L}_i\mathcal{C}_i)\tilde{m}(t) \\ &+ (\mathcal{A}_{di} - \mathcal{L}_j\mathcal{C}_{di})\hat{m}(t - d_1(t)) - (\mathcal{A}_{dj} - \mathcal{L}_j\mathcal{C}_{dj})\hat{m}(t - d_2(t)) \\ &+ (\mathcal{A}_{di} - \mathcal{L}_j\mathcal{C}_{di})\tilde{m}(t - d_1(t)) + \mathcal{B}_{w_i}\omega(t) - \mathcal{B}_i v(t)\} + \bar{\mathcal{G}}\{(f(m, t) - f(\hat{m}, t))\}\} \end{aligned} \tag{32}$$

Therefore, by substituting (31) into (32), we get

$$\dot{\mathcal{T}}_a(m_t, t) \leq -\delta_0 \| s(t) \|, \quad \forall \ \| s(t) \| \neq 0 \tag{33}$$

Consequently, trajectory (7) can drive onto sliding surface $s(t) = 0$, over the finite time. The proof is successfully completed. □

5.2 Design of SMC for the SMO

According to the following *corollary*, the reachability condition can be ensured using *Corollary 1*.

Corollary 2 *With the proper dimension of $\bar{\mathcal{G}}_1$, the sliding mode motion can be obtained for the sliding surface $s_1(t) = 0$ by the following* SMC *law.*

$$\begin{aligned} u(t) &= (\bar{\mathcal{G}}_1\mathcal{B}_j)^{-1}(\sum_{i,j,m=1}^{\ell} \bar{\hbar}_i(\bar{\phi}(t))\bar{\hbar}_j(\bar{\phi}(t)) + \{\bar{\mathcal{G}}_1(\mathcal{B}_j\mathcal{K}_m - \mathcal{L}_i\mathcal{C}_i + \mathcal{L}_j\mathcal{C}_j - \mathcal{L}_j\mathcal{C}_i)\hat{m}(t) \\ &- \mathcal{L}_j\mathcal{C}_{di})\hat{m}(t-d_1(t)) - (\mathcal{A}_{di} - \mathcal{L}_j\mathcal{C}_{dj}))\hat{m}(t-d_2(t)) - \mathcal{L}_j\mathcal{C}_i)\tilde{m}(t)\} \\ &- (\bar{\mathcal{G}}_1\mathcal{B}_j)\{\bar{\mathcal{G}}_1(\mathcal{A}_i - \mathcal{L}_j\mathcal{C}_i + \mathcal{L}_i\mathcal{C}_i)\tilde{m}(t) \\ &- \bar{\mathcal{G}}_1(\mathcal{A}_{di} - \mathcal{L}_j\mathcal{C}_{di})\tilde{m}(t-d_2(t)) - \alpha_i\frac{s_1(t)}{\| s_1(t) \|}\} \end{aligned} \tag{34}$$

where

$$\alpha_i = (\| \bar{\mathcal{G}}_1\mathcal{B}_j \|\| (\bar{\mathcal{G}}\mathcal{B}_j)^{-1} \|)\delta_i + \alpha_0 \tag{35}$$

with α_0 is a positive scalar.

Proof. In this stage, we select the following Lyapunov function

$$\mathcal{T}_b(m_t, t) = \frac{1}{2}s_1(t)^T s_1(t)$$

Computing the time–derivative of $\mathcal{T}_b(m_t, t)$, we get:

$$\begin{aligned} \dot{\mathcal{T}}_b(m_t, t) &= s_1(t)^T\dot{s}_1(t) \\ &= s_1(t)^T\{\bar{\mathcal{G}}_1\sum_{i,j,m=1}^{\ell} \bar{\hbar}_i(\bar{\phi}(t))\hbar_j(\bar{\phi}(t))\{(-\mathcal{B}_j\mathcal{K}_m + \mathcal{L}_i\mathcal{C}_i - \mathcal{L}_j\mathcal{C}_j + \mathcal{L}_j\mathcal{C}_i)\hat{m}(t) + \mathcal{L}_j\mathcal{C}_{di}\hat{m}(t-d_1(t)) \\ &- (\mathcal{A}_{dj} - \mathcal{L}_j\mathcal{C}_{dj})\hat{m}(t-d_2(t)) + \mathcal{L}_j\mathcal{C}_i\tilde{m}(t) + \mathcal{L}_j\mathcal{C}_{di}\tilde{m}(t-d_1(t)) + \mathcal{B}_j(u(t)+v(t))\}\} + \bar{\mathcal{G}}_1 f(\hat{m}, t)) \end{aligned} \tag{36}$$

Substitute the values of (31), (34) and (36), we get

$$\dot{\mathcal{T}}_b(m_t, t) \leq \| s_1(t) \| \sum_{1=1}^{r} \bar{\hbar}_i(\bar{\phi}(t))\{\| \bar{\mathcal{G}}_1\mathcal{B}_j \|\| (\bar{\mathcal{G}}_1\mathcal{B}_i)^{-1} \|)\delta_i - \alpha_0\} \tag{37}$$

Then from (35), we obtained

$$\dot{\mathcal{T}}_b(m_t, t) \leq -\alpha_0(\| s_1(t) \|, \quad \forall \ \| s_1(t) \| \neq 0 \tag{38}$$

Consequently, over the finite time, trajectory (6) can drive onto sliding surface $s_1(t) = 0$. The proof is completed. □

5.3 Algorithm for Controller Design

In this subsection, the authors present some basic steps to calculate the controller and observer gain. Table 1 summarizes the design of an SMO.

Remark 6 *In the present work, relevant issues are addressed using the fuzzy linear matrix inequality (LMI), whose balanced conservation and computation are worth watching and observing. Using Jensen inequality as a measure of integral term, and Lemma 1, conservatism is further intensified. This change is to reduce conservatism to a certain*

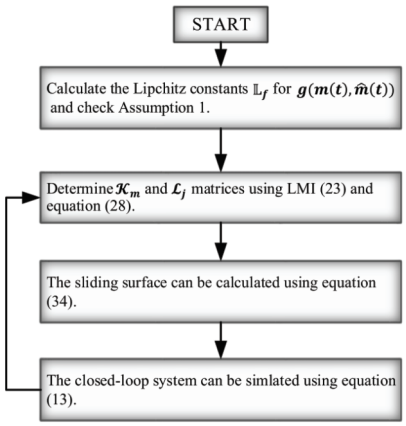

Table 1: Algorithm for controller design.

extent by using the free weighting matrix method. A number of aspects arise from computation, including: (1) As a result of the augmented system, Theorem 1 provides conditions. Dimension matching is required when converting to LMI, which will result in an increase in matrix dimensions. (2) In order to deal with item $\mathcal{C}_i\mathcal{X}_i$, we use an integral inequality and Schur complement that raises in the dimension of the matrix. As a result, we will use less conservatism in the future, and therefore, we will improve methods of control, such as inequality techniques, with stronger controls.

6 Simulation Examples

Example 1: In this section, the effectiveness of the given methods will be tested through simulations of chaotic systems. In order to understand the chaos model, some numerical values are given as

$$(\alpha, \beta, \gamma_1) = (10, 2.7, 28)$$

Let suppose $p_1(t) \in [n_1, n_2]$ and $\dot{p}_1(t) \in [-5, 5]$. Using the *T–S fuzzy system* in (2) with the following system parameters, we can model it as a *chaotic system.*

$$\begin{bmatrix} \mathcal{A}_1 & \mathcal{B}_1 \\ \mathcal{A}_2 & \mathcal{B}_2 \end{bmatrix} = \left[\begin{array}{ccc|cc} -\alpha & \alpha & 0 & 0 & 0 \\ \gamma_1 & -1 & n_1 & 1 & 0 \\ 0 & -n_1 & -\beta & 0 & 1 \\ \hline -\alpha & \alpha & 0 & 0 & 0 \\ \gamma_1 & -1 & n_2 & 1 & 0 \\ 0 & -n_2 & -\beta & 0 & 1 \end{array}\right]$$

An H_∞ performance index of the proposed methods is used to illustrate why they are less conservative than other methods. Using various parameters of α and β, we calculated the minimum attenuation levels as shown in Table 2. There is a significant improvement in efficiency with the proposed method compared with the methods in the references [49], and [50].

6.1 Simulation Example of Power System

Example 2: The electric boat generally consists of two main parts: they are power generation and electric propulsion. The block model of the propulsion system is presented in Figure 2. There are three main parts which are given below:

Table 2: Optimal values of H_∞ performance index.

α		2			5
β	0.3	0.7	0.95	0.8	0.83
[49]	0.191	0.476	12.517	2.888	18.594
[50]	0.252	0.357	0.856	0.653	0.764
Theorem 2	0.187	0.192	0.195	0.317	0.429

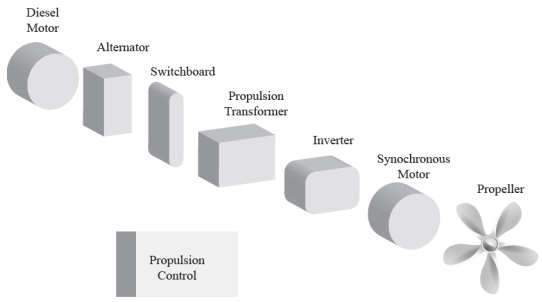

Figure 2: Integrated electric propulsion.

1. Propeller equations.
2. Permanent magnet motor for the synchronous model.
3. Resistance model.

6.2 Propeller equations

First, we write the torque of the propeller and the model of the propulsion as

$$\begin{aligned} \mathbb{T}^{prop} &= \lambda n^2 \mathbb{D}^4 \mathbb{K}^T \\ \mathbb{Q}^{prop} &= \lambda n^2 \mathbb{D}^5 \mathbb{K}^Q \end{aligned} \tag{39}$$

where $\mathbb{K}^Q$ and $\mathbb{K}^T$ present the propeller torque and propeller thrust, respectively. Further, we can write:

$$\begin{aligned} \mathbb{K}^T &= s_1 + s_2 \frac{(1-w)V}{\lambda \mathbb{D}} \\ \mathbb{K}^Q &= r_1 + r_2 \frac{(1-w)V}{\lambda \mathbb{D}} \end{aligned} \tag{40}$$

where

$$\lambda = \frac{\Omega}{2\pi}$$

The equation of vessel motion equation can be written as:

$$m\dot{V} = (1-t)\mathbb{T}^{prop} - \mathbb{R} - \mathbb{T}^{ext} \tag{41}$$

6.3 Resistance model

Second, we will calculate the total resistance of the plant as

$$\mathbb{R} = \mathbb{R}^{air} + \mathbb{R}^{w} + \mathbb{R}^{f} + \mathbb{R}^{app}$$

where $\mathbb{R}^{air}$ is denoted by the air resistance; $\mathbb{R}^{w}$ presents the wave resistance; $\mathbb{R}^{f}$ is the frictional resistance; and $\mathbb{R}^{app}$ is the appendices resistance. By simplifying, the resistance modeled can be written as:

$$\mathbb{R} = aV^2$$

6.4 Permanent Magnet Motor for Synchronous Model (PMMSM)

Permanent magnet voltages for a synchronous motor in the form of equations can be written as:

$$\begin{array}{rcl} v^d & = & \mathbb{R}_s i_d + \mathbb{L}_d \hat{i}_d - p\Omega \mathbb{L}_d i_d \\ v^q & = & \mathbb{R}_s i_q + \mathbb{L}_q \hat{i}_q - p\Omega \mathbb{L}_q i_q \end{array} \tag{42}$$

The mechanical equation can be written as:

$$\mathbb{I}_m \dot{\Omega} = p\Phi^f i_q + p(\mathbb{L}_d - \mathbb{L}_q) i_d i_q - \mathbb{Q}^{prop}$$

where the propeller speed is presented by Ω; $\mathbb{R}_s$ denoted in the stator phase resistance; v^d and v^q are the longitudinal component of stator voltages and the transverse component of stator voltages, respectively; Φ^f is the inductor flux; shaft inertia can be denoted by $\mathbb{I}_m$; i_d and i_q are the stator current longitudinal component and stator current transverse component; $\mathbb{L}_d$ and $\mathbb{L}_q$ are the longitudinal inductance as well as transverse inductance; $\mathbb{Q}^{prop}$ is the propulsion couple; and p is the sign of pole pairs number.

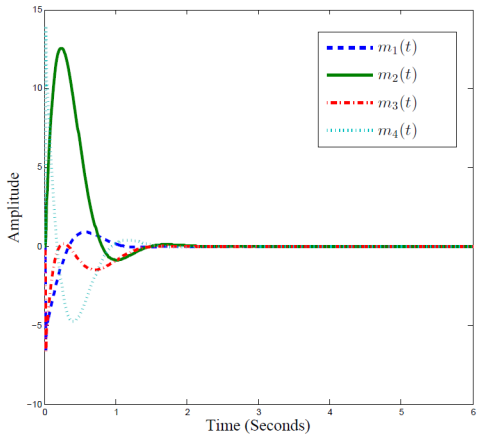

Figure 3: Behaviour for the closed-loop T-S fuzzy system.

The *synchronous motor's* mathematical model for *PM voltages* can be defined as:

$$\begin{array}{rcl} \dot{i}_d & = & \frac{\mathbb{R}_s}{\mathbb{L}_d} i_d + p\Omega \frac{\mathbb{R}_s}{\mathbb{L}_d} i_q + \frac{1}{\mathbb{L}_d} u_q \\ \dot{i}_q & = & \frac{\mathbb{R}_s}{\mathbb{L}_d} i_q - p\Omega \frac{\mathbb{R}_s}{\mathbb{L}_d} i_q - p\Phi^f \Omega + \frac{1}{\mathbb{L}_d} u_q \\ \dot{\Omega} & = & [p\frac{1}{\mathbb{I}_m}(\mathbb{L}_d - \mathbb{L}_q) i_d i_q + p\Phi^f i_q - \frac{1}{4\pi^2}\rho\Omega^2\mathbb{D}^5 r_1 - \frac{1}{2\pi}\rho\Omega\mathbb{D}^4 r_2(1-w)V] \\ \dot{V} & = & \frac{1}{m}[-aV^2 + \frac{1}{4\pi^2}(1-t)\rho\Omega^2\mathbb{D}^4 s_1 + \frac{1}{2\pi}\rho\Omega\mathbb{D}^3 r_2(1-t)(1-w)V] \end{array} \tag{43}$$

Let $m = \begin{bmatrix} m_1 & m_2 & m_3 & m_4 \end{bmatrix}^T = \begin{bmatrix} i_d & i_q & \Omega & V \end{bmatrix}^T$, while in the output $y(t)$ and control signal $u(t)$, we considered the i_q and u_q, respectively. For the feasibility, we assume the ship's electric propulsion system over the domain $m_1(t) \in [d_1, d_2]$, $m_2(t) \in [k_1, k_2]$, and $m_3(t) \in [l_1, l_2]$. Using the approach to construct the *delayed T–S fuzzy system*, we get:

$$\begin{array}{rcl} \dot{m}(t) & = & \sum_{i=1}^{2} \bar{h}_i(\bar{\vartheta}(t))\{\mathcal{A}_i m(t) + \mathcal{A}_{di} m(t - d_1(t)) \\ & + & \mathcal{B}_i u(t) + \mathcal{B}_{\omega i}\omega(t)\} \\ z(t) & = & \sum_{i=1}^{2} \bar{h}_i(\bar{\vartheta}(t))\{\mathcal{E}_i m(t) + \mathcal{E}_{di} m(t - d_1(t))\} \\ y(t) & = & \sum_{i=1}^{2} \bar{h}_i(\bar{\vartheta}(t))\{\mathcal{C}_i m(t) + +\mathcal{C}_{di} m(t - d_1(t))\} \end{array} \tag{44}$$

Algorithm 1 Calculation of Controllers and Observers Gains.

Input: Initial the system parameters according to the system (2) which are $\mathcal{A}_i$, $\mathcal{A}_{di}$, $\mathcal{B}_i$, $\mathcal{E}_i$, $\mathcal{E}_{di}$, $\mathcal{C}_i$, and $\mathcal{C}_{di}$, in accordance with their membership functions and system matrixes.

Delay definition: Then chose $d_{\bar{k}}(t)$, $\bar{k} = 1, 2$ and $\mu_{\bar{k}}$ which have been given as an explicit form and have the upper bound delays.

Stability condition: Check the conditions of *LMIs* in Theorem 2 can be implemented using the prescribed parameters.

Software such as Matlab can be used for this purpose. Alternatively, if *LMIs* cannot be computed, update the parameter in pervious step.

if $t_{min} > 0$ **then**

update the stability criteria of *LMIs* (21)–(26).

else

change the upper bound delay of time–varying function.

end if

Output: Using the values of $\mathcal{Y}_j$, and $\mathcal{X}_i$, get the gains for controllers and observers from the equation (27).

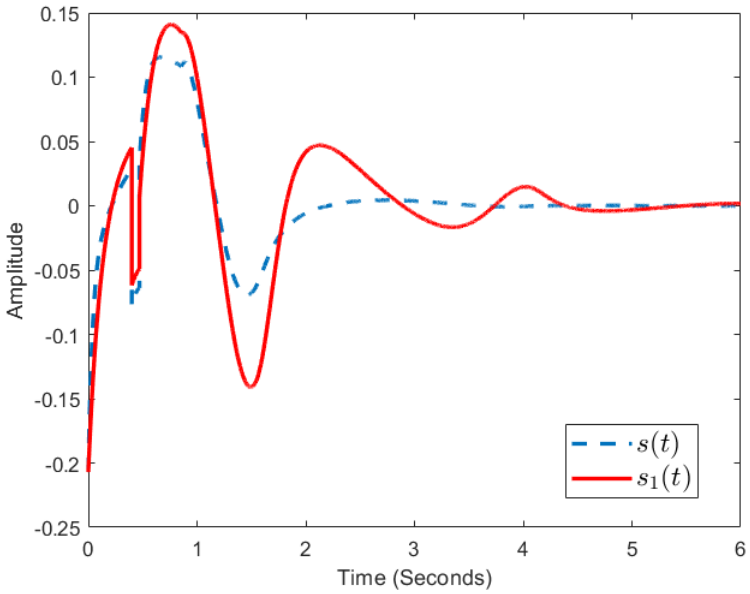

Figure 4: Sliding surfaces $s(t)$ and $s_1(t)$

.

where

$$\mathcal{A}_1 = \begin{bmatrix} a_{11} & a_{12} & 0 & a_{14} \\ a_{21} & a_{22} & 0 & 0 \\ 0 & 0 & \frac{-\mathbb{R}_s}{\mathbb{L}_d} & \frac{pl_2\mathbb{L}_q}{\mathbb{L}_d} \\ -\frac{p\Phi^f}{\mathbb{L}_q} & 0 & -\frac{pl_2\mathbb{L}_d}{\mathbb{L}_q} & -\frac{\mathbb{R}_s}{\mathbb{L}_q} \end{bmatrix}, \quad \mathcal{A}_2 = \begin{bmatrix} b_{11} & b_{12} & 0 & b_{14} \\ b_{21} & b_{22} & 0 & 0 \\ 0 & 0 & \frac{-\mathbb{R}_s}{\mathbb{L}_d} & \frac{pl_2\mathbb{L}_q}{\mathbb{L}_d} \\ -\frac{p\Phi^f}{\mathbb{L}_q} & 0 & -\frac{pl_2\mathbb{L}_d}{\mathbb{L}_q} & -\frac{\mathbb{R}_s}{\mathbb{L}_q} \end{bmatrix}$$

$$\mathcal{A}_{d1} = \begin{bmatrix} c_{11} & c_{12} & 0 & c_{14} \\ c_{21} & c_{22} & 0 & 0 \\ 0 & 0 & \frac{-\mathbb{R}_s}{\mathbb{L}_d} & \frac{pl_2\mathbb{L}_q}{\mathbb{L}_d} \\ -\frac{p\Phi^f}{\mathbb{L}_q} & 0 & -\frac{pl_1\mathbb{L}_d}{\mathbb{L}_q} & -\frac{\mathbb{R}_s}{\mathbb{L}_q} \end{bmatrix}, \quad \mathcal{A}_{d2} = \begin{bmatrix} d_{11} & d_{12} & 0 & d_{14} \\ d_{21} & d_{22} & 0 & 0 \\ 0 & 0 & \frac{-\mathbb{R}_s}{\mathbb{L}_d} & \frac{pl_1\mathbb{L}_q}{\mathbb{L}_d} \\ -\frac{p\Phi^f}{\mathbb{L}_q} & 0 & -\frac{pl_1\mathbb{L}_d}{\mathbb{L}_q} & -\frac{\mathbb{R}_s}{\mathbb{L}_q} \end{bmatrix}$$

$$a_{11} = \frac{-\rho\mathbb{D}^5 r_1 l_2}{4\pi^2 \mathbb{I}_m}, \quad a_{12} = \frac{-\rho\mathbb{D}^4 r_2 l_2 (1-w)}{2\pi\mathbb{I}_m}, \quad a_{14} = \frac{p\Phi^f + p(\mathbb{L}_d - \mathbb{L}_q)d_2}{\mathbb{I}_m}$$

$$
\begin{aligned}
a_{21} &= \frac{(1-t)s_1\rho\mathbb{D}^4 l_2}{4\pi^2 m}, \quad a_{22} = \frac{-2\pi a k_2 + (1-t)(1-w)s_2\rho\mathbb{D}^3 l_2}{2\pi m} \\
b_{11} &= \frac{-\rho\mathbb{D}^5 r_1 l_2}{4\pi^2 \mathbb{I}_m}, \quad b_{12} = \frac{-\rho\mathbb{D}^4 r_2 l_2 (1-w)}{2\pi \mathbb{I}_m}, \quad b_{14} = \frac{p\Phi^f + p(\mathbb{L}_d - \mathbb{L}_q)d_1}{\mathbb{I}_m} \\
b_{21} &= \frac{(1-t)s_1\rho\mathbb{D}^4 l_2}{4\pi^2 m}, \quad b_{22} = \frac{-2\pi a k_2 + (1-t)(1-w)s_2\rho\mathbb{D}^3 l_2}{2\pi m} \\
c_{11} &= \frac{-\rho\mathbb{D}^5 r_1 l_1}{4\pi^2 \mathbb{I}_m}, \quad c_{12} = \frac{-\rho\mathbb{D}^4 r_2 l_1 (1-w)}{2\pi \mathbb{I}_m}, \quad c_{14} = \frac{p\Phi^f + p(\mathbb{L}_d - \mathbb{L}_q)d_2}{\mathbb{I}_m} \\
c_{21} &= \frac{(1-t)s_1\rho\mathbb{D}^4 l_1}{4\pi^2 m}, \quad c_{22} = \frac{-2\pi a k_1 + (1-t)(1-w)s_2\rho\mathbb{D}^3 l_1}{2\pi m} \\
d_{11} &= \frac{-\rho\mathbb{D}^5 r_1 l_1}{4\pi^2 \mathbb{I}_m}, \quad d_{12} = \frac{-\rho\mathbb{D}^4 r_2 l_1 (1-w)}{2\pi \mathbb{I}_m}, \quad d_{14} = \frac{p\Phi^f + p(\mathbb{L}_d - \mathbb{L}_q)d_1}{\mathbb{I}_m} \\
d_{21} &= \frac{(1-t)s_1\rho\mathbb{D}^4 l_1}{4\pi^2 m}, \quad d_{22} = \frac{-2\pi a k_1 + (1-t)(1-w)s_2\rho\mathbb{D}^3 l_1}{2\pi m} \\
\mathcal{C}_1 &= \begin{bmatrix} 1 & 0 & 0 & 0 \end{bmatrix}, \quad \mathcal{C}_2 = \begin{bmatrix} 0 & -0.5 & 0 & 0 \end{bmatrix} \\
\mathcal{C}_{d1} &= \begin{bmatrix} -0.5 & 0 & 1 & 0 \end{bmatrix}, \quad \mathcal{C}_{d2} = \begin{bmatrix} 0 & -0.04 & 0 & -0.02 \end{bmatrix} \\
\mathcal{E}_1 &= \begin{bmatrix} 0 & 1 & 0 & 0 \end{bmatrix}, \quad \mathcal{E}_2 = \begin{bmatrix} 0 & 1.5 & 0 & 0 \end{bmatrix} \\
\mathcal{E}_{d1} &= \begin{bmatrix} 0 & 4.9 & -2 & 0.04 \end{bmatrix}, \quad \mathcal{E}_{d2} = \begin{bmatrix} 0 & 4.9 & -2.5 & 0.04 \end{bmatrix} \\
\mathcal{B}_1 &= \mathcal{B}_2 = \mathcal{B} = \begin{bmatrix} 0 & 0 & \frac{1}{\mathbb{L}_d} & 0 \end{bmatrix}^T \\
\bar{\mathcal{G}} &= \begin{bmatrix} 0 & 0 & -4.95 & 0 \end{bmatrix}, \quad \bar{\mathcal{G}}_1 = \begin{bmatrix} 0 & 0 & 0 & -0.45 \end{bmatrix}
\end{aligned}
$$

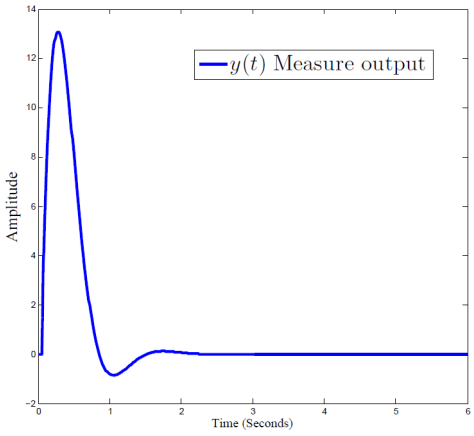

Figure 5: Response of measured output $y(t)$.

Select the same numerical values as [48] given in Table 3. The membership functions for the nonlinear plant are as follows:

$$\bar{h}_1(\bar{\vartheta}(t)) = \frac{\cos(2m_1) + 0.5}{2}, \quad \bar{h}_2(\bar{\vartheta}(t)) = 1 - \bar{h}_1(\bar{\vartheta}(t)) \tag{45}$$

The nonlinear term $f(m,t)$ and $f(\hat{m},t)$ are $-0.35\sin(m_1(t))$ and $-0.65\sin(m_1(t))$, respectively. For time-varying delay, we assume the following function:

$$d_{\bar{k}}(t) = \frac{\bar{d}_{\bar{k}} + \bar{d}_{\bar{k}}\sin(2\mu_i t/\bar{d}_{\bar{k}})}{2}, \qquad \bar{k} = 1, 2.$$

where $(\bar{d}_1, \bar{d}_2) = (0.65, 0.75)$ and $(L_f, k, \mu_1, \mu_2) = (0.45, 0.55, 0.22, 0.47)$.
For the observer controller, the following are the membership functions:

Table 3: Propulsion parameters of *PMMSM*

Unit name	Symbol	Numerical values
Wake fraction	w	0.2304
Inductance (Longitudinal)	$\mathbb{L}_d$	0.0060
Inductance (Transversal)	$\mathbb{L}_d$	0.0059
Thrust coefficient	s_1 & s_2	(0.5,-1.1)
Torque coefficient	r_1 & r_2	(0.075,-0.1375)
Nominal torque & thrust	$\mathbb{Q}_n$ & $\mathbb{T}_n$	(3.14800 $\times$ 10^5 Nm,3.82000 $\times$ 10^5 N)
Voltage	V	4.160 KV.
Number of pair poles	p	4.
Power of motor	S	5 MVA.
Water density	ρ	1025 kg/m^3.
Stator resistance	$\mathbb{R}_s$	0.0148.
Weight of ship	m	20690 tonnes.
Coefficient of resistance	a	4.7 $\times$ 10^3.
Diameter of propeller	$\mathbb{D}$	5.9 m.

$$\bar{\hbar}_1(\bar{\phi}(t)) = 0.99 \exp^{\frac{-\hat{m}^2(t)}{2\times 1.5^2}}, \quad \bar{\hbar}_2(\bar{\phi}(t)) = 1 - \bar{\hbar}_1(\bar{\phi}(t)) \tag{46}$$

Furthermore, $w(t) = \frac{1}{0.75+1.75t}$, $t \geq 0$ is assumed to be the external disturbance. The initial condition will be as $\tilde{\varphi}(t) = [1, -3, 5, -7]^T$, the *T–S fuzzy system's* state responses (2) in the parameters given in (44). We will examine the designs for Passive and dissipative control issues.

Remark 7 *External disturbances will have an impact on a system's stability. Performance indicators can be determined by analyzing the system, which can lead to a more stable system. For system analysis, standard single performances are used. Extended dissipative performance can be converted into four general single performances by adjusting weighting matrices and scalars. These allow a systematic analysis to be as broad and comprehensive as*

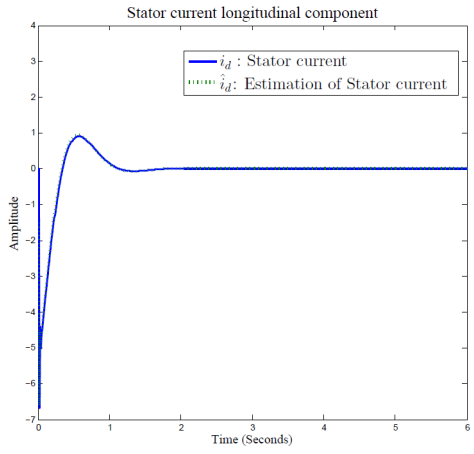

Figure 6: The trajectory of stator current and its estimation (Longitudinal component).

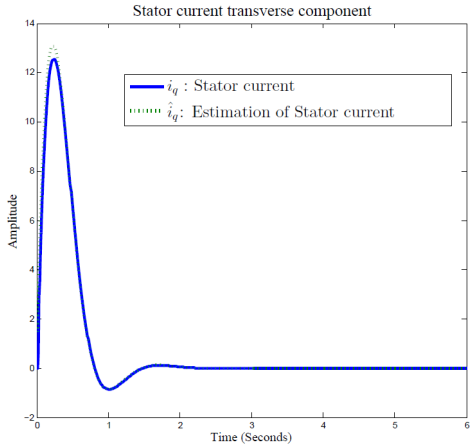

Figure 7: The trajectory of stator current and its estimation (Transverse component).

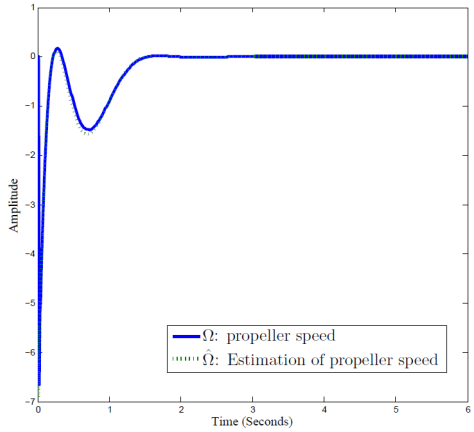

Figure 8: Path of propeller speed Ω and its estimation $\hat{\Omega}$.

possible.

Table 4: Case-specific matrices.

Analysis	Γ_0	Γ_1	Γ_2	Γ_3
Dissipativity	0	-1	1	γ
$L_2 - L_\infty$	1	0	0	γ^2
Passivity	0	0	1	γ
H_∞ performance	0	-1	0	γ^2

Passive Control: According to the matrices parameters in Table 2 for passive control, with $\gamma = 3.75$. Furthermore, we can find the *LMIs* using Algorithm 1 for (21)–(26) that are feasible and they lead to the following feasible solutions:

$$\begin{bmatrix} \mathcal{K}_1 \\ \mathcal{K}_2 \end{bmatrix} = \begin{bmatrix} -0.0003 & -0.0051 & -0.1886 & 0.0001 \\ -0.0018 & -0.0050 & -0.2632 & 0.0036 \end{bmatrix}$$

$$\begin{bmatrix} \mathcal{L}_1 \\ \mathcal{L}_2 \end{bmatrix}^T = \begin{bmatrix} -0.0169 & 0.1015 & -0.0293 & -0.0546 \\ 0.0278 & 0.0208 & 0.0884 & 0.0441 \end{bmatrix}^T$$

According to *LMIs* of *Theorem 2*, the passive control parameters can be obtained using (27). Let's assume the initial conditions for the observer–state as $\tilde{\varphi}_o(t) = [1.15, -3.5, 5.45, -7.75]^T$. Figure 3 presents the state trajectories for

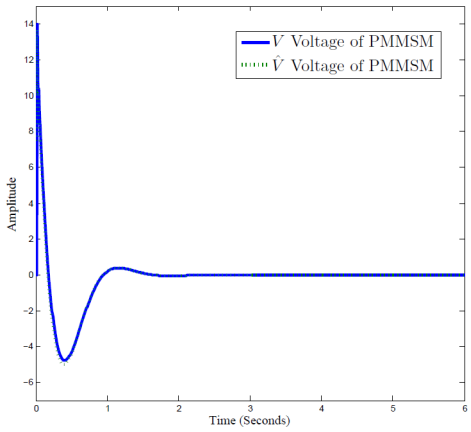

Figure 9: Path of the voltage of *PMMSM* "V" and its estimation "$\hat{V}$".

the closed–loop system. In the power sector, it is necessary to keep the states of the nonlinear model, that's why we also explore the properties of observer-based states which are exhibited in above-mentioned Figures. These figures, not only show stability but have finally approached zero. In addition, Figures 4 and 5 present the behaviour curves for the sliding surfaces $s(t)$ and $s_1(t)$, and measured output $y(t)$, respectively. Based on these simulation results, we can conclude that the synthetic *T–S fuzzy* controller is capable of meeting the requirements.

Remark 8 *To show the less conservative results, we made a comparison which is given in Table 3. We borrowed the example from the Reference [43], in which authors used the anti-windup compensator for the stability analysis. Hence, we discuss the same problem numerically. Our next step is to compare the maximum allowable upper bound delay for those methods suggested in [43], [44], and our paper. Table 5 presents the comparison, where* $\bar{d} = \bar{d}_i$, $i = 1, 2$. *According to the table, our methods are less than those obtained with Refs. [43], and [44], for the upper bound delay. The method described in this study is less conservative than the methods proposed in Refs. [43], and [44].*

Table 5: Maximum Upper bound delay $\bar{d}_i = \bar{d}$ under $(\rho_1, \rho_2) = 100$.

Method	$\bar{d}$
[43]	3.15
[44]	6.56
Theorem 2	11.82

Dissipative Control: According to the matrices in Table 2 parameters of dissipative control, with $\gamma = 4.25$. Furthermore, we can find the *LMIs* using Algorithm 1 for (21)–(26) that are feasible and they lead to the following reasonable solutions:

$$\begin{bmatrix} \mathcal{K}_1 \\ \mathcal{K}_2 \end{bmatrix} = \begin{bmatrix} 1.6033 & -0.7561 & 0.0310 & -0.8013 \\ 1.6734 & -0.7989 & 0.0318 & -0.8662 \end{bmatrix}$$

$$\begin{bmatrix} \mathcal{L}_1 \\ \mathcal{L}_2 \end{bmatrix}^T = \begin{bmatrix} -6.7807 & -1.9158 & 0.6283 & -0.9491 \\ -6.5050 & -1.7785 & 0.4771 & -0.8880 \end{bmatrix}^T$$

According to the simulation analysis, Figure 6 presents the trajectory of the stator current and its estimation for the *longitudinal component*, while Figure 7 shows the behaviour of the stator current and its estimation for the *transverse component*. In the same consequences, Figures 8 and 9 exhibit the propeller speed and voltage of *PMMSM* and their estimation, respectively. Moreover, Figure 10 illustrates that the control law responds with nonlinear input.

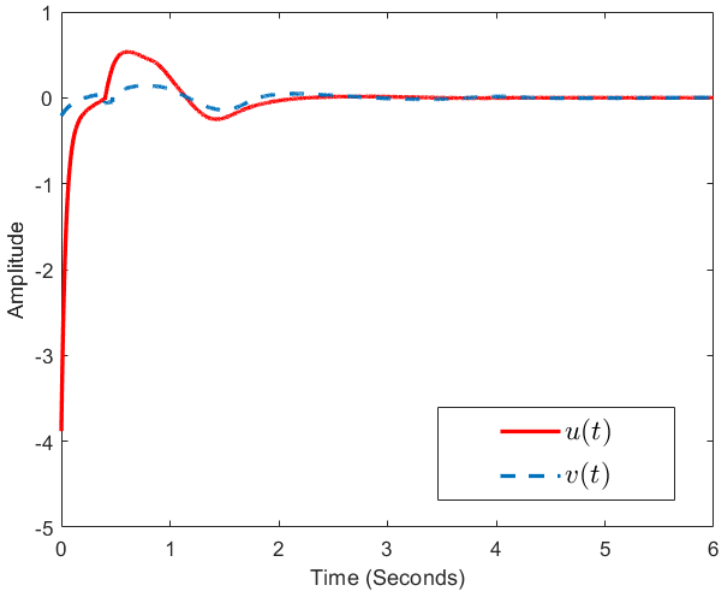

Figure 10: Response of the control input $u(t)$ and nonlinear input $v(t)$.

The dissipativity of an energy system refers to the ratio between the energy supply from the outside and the energy stored inside. It is therefore a very important consideration when designing electrical circuits. Because of this, we analyzed these circuits in our article.

Remark 9 *This research will further extend to distributed sensor filtering. In distributed sensors, each sensor node will need to collect data from the other sensors, compare it with the other values, and transmit it through communication. From this aspect, we will explore various issues, such as power supply and synchronization. Thus, it will be imperative to elaborate on which target plant needs the proposed theoretical approach. In view of the sampled control system, it has many industrial applications e.g., Power systems, Mechanical plants, Manufacturing systems, and Communication systems. Dissipativity is simply the ratio of input to output energy in systems with multiple energy sources.*

Remark 10 *In the simulation section, the authors focused only on two kinds of control analysis, namely passive control and dissipative control. These kinds of control are very essential for the power system and mechanical systems. As a result, dissipation is a crucial aspect of electrical circuits. Our research area includes these investigations for this reason.*

7 Conclusion

We discuss a continuous-time nonlinear model-based control system with sliding mode control. A new observer model was developed to account for the presence of state and observer delays. A concept of dissipative control also provides an analysis of the performance of H_∞, L_2-L_∞, dissipativity, and passivity within a unified framework. Based on the new Lyapunov stability theory, the new error *SMO* system constructed has been conditionally stabilized, as well as analyzed for extended dissipative performance. By using the controlled sliding mode law, the system state can also converge on the sliding surface. Following that, we solve the matrix convex optimization problem in order to find the gains in the sliding mode controller and observer. Its feasibility will be demonstrated through the simulation with an engineering application. It can also be applied to more complex systems, including switched networks, multi-time scale networks, fuzzy networks, etc. In addition to the effect of cyber-attacks on information distribution, which we will study in the future.

References

[1] J. Li, G. Zhang, C. Liu and W. Zhang. COLREGs–Constrained Adaptive Fuzzy Event–Triggered Control for Underactuated Surface Vessels With the Actuator Failures, *IEEE Transactions on Fuzzy Systems*, vol. 29, no. 12, pp: 3822–3832, 2021.

[2] X. Shao and D. Ye. Fuzzy Adaptive Event-Triggered Secure Control for Stochastic Nonlinear High–Order MASs Subject to DoS Attacks and Actuator Faults, *IEEE Transactions on Fuzzy Systems*, vol. 29, no. 12, pp: 3812–3821, 2021.

[3] W. Heemels , A.R. Teel , N. Wouw , N. Dragan. Networked control systems with communication constraints: Tradeoffs between transmission intervals, delays and performance, *IEEE Transactions on Automatic control*, vol. 55, no. 8, pp: 1781–1796, 2010.

[4] Y. Wang, X. Hu, K. Shi, X. Song, H. Shen. Network–based passive estimation for switched complex dynamical networks under persistent dwell–time with limited signals, *Journal of Franklin Institute*, vol. 357, no. 15, pp: 10921–10936, 2020.

[5] X. Luan, P. Shi, F. Liu. Stabilization of networked control systems with random delays, *IEEE Transactions on Industrial Electronics*, vol. 58, no. 9, pp: 43923–4330, 2010.

[6] W. Liu, P. Shi, Optimal linear filtering for networked control systems with time-correlated fading channels, *Automatica*, vol. 101, no. 9, pp: 345–353, 2019.

[7] X. Jiang, M. Chi, X. Chen, H. Yan, T. Huang, Tracking and regulation performance limitations of networked control systems over erasure channel with input quantization, *IEEE Transactions on Automatic Control*, vol. 67, no. 9, pp: 4862–4869, 2022.

[8] J. Wang, T. Ru, J. Xia, H. Shen, V. Sreeram. Asynchronous event-triggered sliding mode control for Semi–Markov jump systems within a finite-time interval, *IEEE Translation Circuits System I, Registration Papers*, vol. 68, no. 1, pp: 458–468, 2020.

[9] F. Li , Y. Liu. Adaptive event–triggered output–feedback controller for uncertain nonlinear systems, *Automatica*, vol. 117, 109006, 2020.

[10] H. Shen, M. Dai, Y. Luo, J. Cao, M. Chadli. Fault–tolerant fuzzy control for semi–Markov jump nonlinear systems subject to incomplete SMK and actuator failures, *IEEE Transactions on Fuzzy Systems*, vol. 29, no. 10, pp: 3043–3053, 2020.

[11] H. Shen , Y. Men , Z.G. Wu , J. Cao , G. Lu. Network–based quantized control for fuzzy singularly perturbed semi–Markov jump systems and its application, *IEEE Translation Circuits System I, Registration Papers*, vol. 66, no. 3, pp: 1130–1140, 2019.

[12] Lotfi A. Zadeh, Ali M. Abbasov, Ronald R. Yager, Shahnaz N. Shahbazova, Marek Z. Reformat. Recent Developments and New Direction in Soft-Computing Foundations and Applications, *Selected Papers from the 4th World Conference on Soft Computing*, doi.org/10.1007/978-3-319-32229-2, May 25-27, 2014, Berkeley.

[13] Y. Mi, Y. Song, Y. Fu and C. Wang. The Adaptive Sliding Mode Reactive Power Control Strategy for Wind–Diesel Power System Based on Sliding Mode Observer, *IEEE Transactions on Sustainable Energy*, vol. 11, no. 4, pp: 2241–2251, 2020.

[14] J. Wang, C. Yang, H. Shen, J. Cao, L. Rutkowski. Sliding–mode control for slow–sampling singularly perturbed systems subject to Markov jump parameters, *IEEE Transactions on Systems, Man, and Cybernetics*, vol. 51, no. 12, pp: 7579–7586, 2020.

[15] X. Liu, X. Su, P. Shi, C. Shen, Y. Peng. Event-triggered sliding mode control of nonlinear dynamic systems, *Automatica*, vol. 112, 108738, 2020.

[16] B. Jiang, H. Karimi, Y. Kao, and C. Gao. Takagi–Sugeno model based event–triggered fuzzy sliding mode control of networked control systems with semi–markovian switchings, *IEEE Transactions on Fuzzy Systems*, vol. 28, no. 4, pp: 673–683, 2019.

[17] X. Lin, X. Li, J.H. Park. Output–feedback stabilization for planar output-constrained switched nonlinear systems, *International Journal of Robust Nonlinear Control*, vol. 30, no. 5, pp: 1819–1830, 2020.

[18] H. Li, J. Wang, H. Du, and H. R. Karimi. Adaptive sliding mode control for Takagi–Sugeno fuzzy systems and its applications, *IEEE Transactions on Fuzzy Systems*, vol. 26, no. 2, pp: 531–542, 2018.

[19] X.X. Yin, Y.G. Lin, W. Li, H.W. Liu, and Y.J. Gu. Fuzzy–logic sliding–mode control strategy for extracting maximum wind power, *IEEE Transactions on Energy Conversion*, vol. 30, no. 4, pp: 1267–1278, 2015.

[20] M. Kchaou, H. Gassara and A. E. Hajjaji. Dissipativity–based integral sliding mode control for a class of Takagi–Sugeno fuzzy singular systems with time–varying delay, *IET Control Theory & Applications*, vol. 8, pp: 2045–2054, 2014.

[21] Q. Sun, J. Ren, J. Fu. Robust preview control of uncertain discrete–time T–S fuzzy Markovian jump systems subject to time–varying delays via sliding mode approach, *Information Sciences*, vol. 639, 118980, 2023.

[22] R. Nie, W. Du, Z. Li, S. He. Sliding Mode–based Finite–time Consensus Tracking Control for Multi–agent Systems under Actuator Attacks, *Information Sciences*, https://doi.org/10.1016/j.ins.2023.118971, 118971, 2023.

[23] R. M. Nagarale and B. M. Patre. Exponential function based fuzzy sliding mode control of uncertain nonlinear systems, *International Journal of Dynamics & Control*, vol. 4, pp: 67–75, 2016.

[24] D. B. Salem and W. Saad. Integral sliding mode control for systems with time–varying input and state delays, *International Conference on Engineering & MIS (ICEMIS)*, pp: 978–982, 2017.

[25] Q. Gao, G. Feng, L. Liu, J. B. Qiu, and Y.Wang. Robust H_∞ control for stochastic T–S fuzzy systems via integral sliding–mode approach, *IEEE Transactions on Fuzzy Systems*, vol. 22, no. 4, pp: 870–881, 2014.

[26] H. Pang, Y. Shang, P. Wang. Design of a sliding mode observer–based fault tolerant controller for automobile active suspensions with parameter uncertainties and sensor faults. *IEEE Access*, vol. 8, pp: 186963–186975, 2020.

[27] J. Li and Q. Zhang. An integral sliding mode control approach to observer based stabilization of stochastic Itô descriptor systems, *Neurocomputing*, vol. 173, pp: 1330–1340, 2016.

[28] K. Hfaiedh, K. Dahech, and T. Damak. A sliding mode observer for uncertain nonlinear systems based on multiple modes approach, *International Journal of Automat. Comput.*, vol. 14, no. 2, pp: 202–212, 2017.

[29] H. Yan, H. Zhang, X. Zhan, Y. Wang, S. Chen, F. Yang. Event–triggered sliding mode control of switched neural networks with mode-dependent average dwell time, *IEEE Transactions on Systems, Man, and Cybernetics*, vol. 51, no. 2, pp: 1233–1243, 2020.

[30] R. Li, X. Zhang. Adaptive sliding mode observer design for a class of T–S fuzzy descriptor fractional order systems, *IEEE Transactions on Fuzzy Systems*, vol. 28, no. 9, pp: 1951–1960, 2020.

[31] X. Xie, C. Wei, Z. Gu and K. Shi. Relaxed Resilient Fuzzy Stabilization of Discrete–Time Takagi-Sugeno Systems Via A Higher Order Time–Variant Balanced Matrix Method, *IEEE Transactions on Fuzzy Systems*, vol. 30, no. 11, pp: 5044–5050, 2022.

[32] J. Zhang, X. Liu, Y. Xia, Z. Zuo, Y. Wang. Disturbance observer–based integral sliding–mode control for systems with mismatched disturbances, *IEEE Transactions on Industrial Electronics*, vol. 63, no. 11, pp: 7040–7048, 2016.

[33] J. Linares-Flores et al. Sliding Mode Control Based on Linear Extended State Observer for DC-to-DC Buck–Boost Power Converter System With Mismatched Disturbances, *IEEE Transactions on Industry Applications*, vol. 58, no. 1, pp. 940-950, 2022.

[34] X. Shen et al., Adaptive Second–Order Sliding Mode Control for Grid–Connected NPC Converters With Enhanced Disturbance Rejection, *IEEE Transactions on Power Electronics*, vol. 37, no. 1, pp. 206–220, 2022.

[35] F. Li , Y. Liu , Adaptive event-triggered output-feedback controller for uncertain nonlinear systems, *Automatica*, 117, 109006, 2020.

[36] H. Shen , F. Li , H. Yan , H.R. Karimi , H.K. Lam. Finite–time event–triggered H_∞ control for t-s fuzzy Markov jump systems, *IEEE Transactions on Fuzzy Systems*, Vol. 26, 5, pp: 3122–3135, 2018.

[37] H. Shen, M. Dai, Y. Luo, J. Cao, M. Chadli, Fault–tolerant fuzzy control for semi–Markov jump nonlinear systems subject to incomplete SMK and actuator failures, *IEEE Transactions on Fuzzy Systems*, vol. 29, no. 10, pp: 3043–3053, 2020,

[38] U. M. Al-Saggaf, M. Bettayeb and S. Djennoune. Super–twisting algorithm–based sliding mode observer for synchronization of nonlinear incommensurate fractional–order chaotic systems subject to unknown inputs, *Arabian Journal for Science and Engineering*, vol. 42, pp: 3065–3075, 2017.

[39] P. Cheng, H. Wang, V. Stojanovic, F. Liu, S. He, K. Shi. Dissipativity–based finite–time asynchronous output feedback control for wind turbine system via a hidden Markov model, *International Journal of Systems Science*, vol. 53, no. 15, pp: 3177–3189, 2022.

[40] X. Liang, J. Xia, G. Chen, H. Zhang, Z. Wang. Dissipativity–based sampled–data control for fuzzy Markovian jump systems, *Applied Mathematics and Computation*, vol. 361, pp: 552–564, 2019.

[41] B. Zhang , W.X. Zheng , S. Xu. Filtering of Markovian jump delay systems based on a new performance index, *IEEE Translation Circuits System I, Registration Papers*, vol. 60, no. 5, pp: 1250–1263, 2013.

[42] J. Wang , Z. Huang, Z. Wu, J. Cao, H. Shen. Extended dissipative control for singularly perturbed PDT switched systems and its application, *IEEE Translation Circuits System I, Registration Papers*, vol. 67, no. 12, pp: 5281–5289, 2020.

[43] X. Song, J. Lu, S. Xu, H. Shen, J. Lu. Robust stabilization of state delayed T–S fuzzy systems with input saturation via dynamic anti–windup fuzzy design, *International Journal of Innovative Computing Information Control*, vol. 7, no. 12, pp: 6665–6676, 2011.

[44] K. Naamane, E.H. Tissir. Robust Anti–windup Controller Design for Takagi–Sugeno Fuzzy Systems with Time–Varying Delays and Actuator Saturation, *Circuits, Systems, and Signal Processing*, vol. 41, pp: 1426–1452, 2022.

[45] B. Zhang, W. X. Zheng, and S. Xu. Filtering of Markovian jump delay systems based on a new performance index. *IEEE Transactions on Circuits and Systems-I: Regular Papers*, vol. 60, no. 5, pp. 1250–1263, 2013.

[46] C. Peng, S. Ma, and X. Xie, Observer–Based Non–PDC Control for Networked T–S Fuzzy Systems With an Event–Triggered Communication, *IEEE Transactions on Cybernetics*, vol. 47, no. 8, pp, 2279–2287, 2017.

[47] Y. Yang, Y. He. Non–fragile observer–based robust control for uncertain systems via aperiodically intermittent control, *Information Sciences*, vol. 573, pp: 239–261, 2021.

[48] L. Qiao, Y. Yang. Fault–tolerant control for T–S fuzzy systems with sensor faults: Application to a ship propulsion system, *Journal of the Franklin Institute*, vol. 355, no. 12, pp: 4854–4872, 2018.

[49] M. Kchaou. Robust H_∞ observer–based control for a class of (T–S) fuzzy descriptor systems with time–varying delay, *International Journal of Fuzzy Systems*, vol. 19, pp: 909–924, 2017.

[50] Y. Yang, M. Zheng. Sampled–data control for a class of singular takagi–sugeno fuzzy systems with application in truck–trailer system, *Symmetry*, vol. 14, no. 9, 1762, 2022.